

**WASTE HEAT RECOVERY FROM AN IDEAL MOLTEN
CARBONATE FUEL CELL USING REHEAT AND
REGENERATIVE BRAYSSON CYCLE**

A PROJECT REPORT SUBMITTED IN PARTIAL FULFILLMENT OF THE
REQUIREMENT FOR THE AWARD OF THE DEGREE OF BACHELOR OF
TECHNOLOGY IN MECHANICAL ENGINEERING

SUBMITTED BY

P. SREE MANOJ	317126520107
D. AKHIL	317126520076
S. KEERTHI TEJA	317126520117
P.J. SWAROOP	318126520L21
M. MANASA	317126520096

UNDER THE ESTEEMED GUIDANCE OF

Mr. R. CHANDRAMOULI M.Tech , Associate Professor.



**DEPARTMENT OF MECHANICAL ENGINEERING
ANIL NEERUKONDA INSTITUTE OF TECHNOLOGY &
SCIENCES (AUTONOMOUS)**

**(Permanently Affiliated to Andhra University, Approved by AICTE, and
Accredited by NBA & NAAC with 'A' grade) SANGIVALASA
BHEEMUNIPATNAM (MANDAL) - 531162
VISAKHAPATNAM (DIST.), ANDHRA PRADESH, INDIA.**

ANIL NEERUKONDA INSTITUTE OF TECHNOLOGY & SCIENCES (A)

(Affiliated to Andhra University, Approved by AICTE, Accredited by NBA & NAAC with A grade)

SANGIVALASA, VISAKHAPATNAM (District) – 531162



CERTIFICATE

This is to certify that the Project Report entitled “**WASTE HEAT RECOVERY FROM AN IDEAL MOLTEN CARBONATE FUEL CELL USING REHEAT AND REGENERATIVE BRAYSSON CYCLE**” being submitted by PANUTHULA SREE MANOJ (317126520107), DUNNA AKHIL (317126520076), SIRRA KEERTHI TEJA (317126520117), PUDI JYOTHI SWAROOP (318126520L21), MATHE MANASA (317126520096) in partial fulfillments for the award of degree of **BACHELOR OF TECHNOLOGY in MECHANICAL ENGINEERING**. It is the work of bona-fide, carried out under the guidance and supervision of **MR.R.CHANDRA MOULI**, Associate Professor, Department Of Mechanical Engineering, ANITS during the academic year of 2017-2021.

PROJECT GUIDE

(MR.R.CHANDRA MOULI)
Associate Professor
Mechanical Engineering Department
ANITS, Visakhapatnam.

Approved By

HEAD OF THE DEPARTMENT

(Dr. B. Naga Raju)
Head of the Department
Mechanical Engineering Department
ANITS, Visakhapatnam.

ACKNOWLEDGEMENT

We express immensely our deep sense of gratitude to **Mr.R. Chandramouli, M.Tech , Associate Professor, M.S.S Srinivas Rao, Sr. Assistant Professor,** Department of Mechanical Engineering, **Dr.M. Shiva Naresh, Assistant Principal, Dr.S. Siva Kumar, Assistant Professor,** Department of Chemistry, and **P.Mallika Rani , Assistant professor,** Department of Chemical Engineering ,Anil Neerukonda Institute of Technology & Sciences, Sangivalasa, Bheemunipatnam (mandal), Visakhapatnam District for their valuable guidance and encouragement at every stage of the work made it a successful fulfilment.

We were very thankful to our **Professor T.V. HANUMANTH RAO,** Principal, ANITS and **Professor B. NAGA RAJU,** Head of the Department, Mechanical Engineering, Anil Neerukonda Institute of Technology & Sciences for their valuable suggestions and also for encouraging us.

Last but not least, we would like to convey our thanks to all who have contributed either directly or indirectly for the completion of work.

P. Sree Manoj (317126520107)

D. Akhil (317126520076)

S. Keerthi Teja (317126520117)

P.J Swaroop (318126520L21)

M. Manasa (317126520096)

ABSTRACT

Direct energy conversion devices are gaining prominence by virtue of their high efficiency. This is in fact due to the conversion of chemical energy directly into electrical energy without passing through the thermal energy phase. Fuel cells, Photovoltaic cells are few examples of Direct energy conversion devices, which have received recognition in terms of research and also practical usage. Fuel cells work on the principle of chemical reaction between the fuels like Hydrogen, Methane, propane, ammonia etc and an oxidiser. Fuel cells generally possess high first and second law efficiencies and are finding applications in remote areas like submarines, spacecrafts etc.

The exothermic reaction in the fuel cell produces an enormous quantity of heat which is dissipated to the surroundings. The working temperature of fuel cell is very high and are in the order of 600 – 700°C. The exergy associated with the waste heat is colossal and is simply lost to the atmosphere. Generally, waste heat liberated from the fuel cells was used to generate power by running the Brayton (or) Rankine cycle. But in 1997, T H Frost first proposed an Ideal Braysson cycle whose efficiency is much higher than the Brayton cycle. In this project, a combined system of Methane (fuel)-Potassium Carbonate (oxidiser) Molten Carbonate Fuel Cell, reheat and regenerative Braysson cycle are used in order to recover the waste heat. Energy and Exergy based evaluation of this combined system is carried out in this work.

In the analysis, Molten Carbonate Fuel Cell is assumed to operate at 650° C and the turbine inlet temperature (TIT) range of Braysson cycle is assumed as 400 to 600°C. It has been observed that there exist different optimum pressure ratio values for maximum power output and maximum efficiencies. Both the energy and exergy efficiencies of the combined cycle increases with the increase in turbine inlet temperature.

It is further observed that energy and exergy efficiencies of the fuel cell are independent of turbine inlet temperature and pressure ratio. The power obtained from the fuel cell is 9 to 16 times higher than the power obtained from the waste heat through Braysson depending on the pressure ratio and TIT. The combined system depicts energy efficiency in the range of 73% to 76% and that of the fuel cell is about 65%. Exergy destruction rates for the individual equipment and the total system are also obtained as a function of pressure ratio and TIT. The exergy destruction rates are found to be maximum in the heat transfer equipment and minimum in the fuel cell.

The waste heat from the Molten Carbonate Fuel Cell is found to be 1354.6 KW at turbine inlet temperature of 600°C and at an optimum pressure ratio of 1.4. The power output of reheat and regenerative Braysson cycle obtained by recovering this waste heat is found to be nearly 580 KW.

CONTENTS

Sl.No	Description	Page No.
CHAPTER 1: INTRODUCTION		
1.1	Energy	1
1.2	Laws of Thermodynamics and their Significance	2
	1.2.1 First law of thermodynamics	3
	1.2.2 Second law of thermodynamics	3
1.3	Exergy	4
	1.3.1 Exergy analysis	5
	1.3.2 Energy balance for steady flow system	5
1.4	Second law of Efficiency (or) Exergy Efficiency	6
1.5	Fuel cell	6
	1.5.1 History	7
	1.5.2 Types	8
	1.5.3 Applications	10
	1.5.4 Advantages and Disadvantages	10
1.6	Evolution of Braysson Cycle	11
	1.6.1 Brayton Cycle	12
	1.6.2 Ericsson cycle	13
	1.6.3 Concept of ideal cycle	14
1.7	Reheat & Regenerative Braysson Cycle	15
	1.7.1 Regeneration	15
	1.7.2 System description	15
	1.7.2.1 Polytropic expansion	17
	1.7.2.2 Regeneration	17
	1.7.2.3 Isobaric heat addition	17
	1.7.2.4 Polytropic expansion	17
	1.7.2.5 Isobaric heat addition in reheater	17
	1.7.2.6 Regeneration at constant pressure	18
	1.7.2.7 isobaric heat rejection	18
	1.7.2.8 Isothermal heat rejection	18
CHAPTER 2: LITERATURE REVIEW and SCOPE OF LITERATURE WORK		20
CHAPTER 3: THERMODYNAMIC ANALYSIS		26
3.1	System Description	27
3.2	Energy analysis	28
	3.2.1 Isentropic compression	28
	3.2.2 Isentropic expansion	28
	3.2.3 Regeneration	29
	3.2.4 Isothermal heat rejection using multi-stage compressor	29

3.3	Exergy analysis	31
	3.3.1 Isentropic compression	31
	3.3.2 Regeneration	31
	3.3.3 Fuel cells 1 & 2	32
	3.3.4 Heating of fluid	32
	3.3.5 Isentropic Expansion	32
	3.3.6 Cooler	33
	3.3.7 Multi-stage Compressor	33
	3.3.8 Exergy Efficiency of combined system	33
	CHAPTER 4: RESULT AND DISCUSSIONS	34
	CHAPTER 5: CONCLUSIONS & FUTURE SCOPE	50
	CHAPTER 6:	52
	ENVIRONMENTAL IMPACTS	53
	AND	
	SUSTAINABLE DEVELOPMENT	54
	REFERENCES	55
	APPENDIX	57

LIST OF FIGURES

Fig no.	Title	Page no.
1.1	MCFC Fuel cell	7
1.2	Layout of Braysson cycle with cooler and multi stage compressor	11
1.3	Layout of a Brayton cycle with P-V & T-S plot	12
1.4	P-V & T-S plot for an Ericsson cycle	13
1.5	T-S plot for an ideal Braysson cycle	14
1.6	Schematic diagram of Braysson cycle with reheat and regeneration and T-S diagram for Reheat & Regenerative Braysson cycle	16
3.1	T-S diagram for Reheat & Regenerative Braysson cycle	27
4.1	Energy efficiency of Reheat and Regenerative Braysson cycle vs. Pressure ratio for different TIT	36
4.2	Exergy efficiency of Reheat and Regenerative Braysson cycle vs. Pressure ratio for different TIT	36
4.3	Energy efficiency of Fuel Cell vs. Pressure Ratio for different TIT	38
4.4	Exergy efficiency of Fuel Cell vs. Pressure Ratio for different TIT	38
4.5	Power Output of Reheat & Regenerative Braysson Cycle vs. Pressure Ratio for different TIT	39
4.6	Power Output of Fuel Cell vs. Pressure Ratio for different TIT	40
4.7	Net power output of combined system (KW) vs Pressure ratio for different TIT	41
4.8	Power Ratio (Fuel cell/Braysson) vs. Pressure Ratio for different TIT	42
4.9	Specific Fuel Consumption of combined system (Kg/KW-hr) vs. Pressure Ratio for different TIT	43
4.10	Energy Efficiency of combined system (%) vs. Pressure Ratio for different TIT	44
4.11	Exergy Efficiency of combined system (%) vs. Pressure Ratio for different TIT	44
4.12	Energy Efficiency (%) vs Pressure Ratio	45
4.13	Pie chart representing Component wise exergy destruction rates at an optimum pressure ratio of 1.4 and TIT = 600 °C	46
4.14	Total Exergy Destruction vs Pressure ratio at different TIT	47

NOMENCLATURE

e_{ch_4} = chemical exergy of CH₄ (KJ/Kg)

e_{co} = chemical exergy of K₂CO₃(KJ/Kg)

c_p =specific heat of helium = 5.19 (KJ/Kg-K)

e_x = exergy at point x (KJ/Kg)

$\dot{m}_{h_2o_1}$ = mass flow rate of water in fuel cell-1 (Kg/s)

$\dot{m}_{h_2o_2}$ = mass flow rate of water in fuel cell-2 (Kg/s)

$\dot{m}_{f_{CH_4_1}}$ = mass flow rate of methane in Fuel cell-1 (Kg/s)

$\dot{m}_{f_{CH_4_2}}$ = mass flow rate of methane in Fuel cell-2 (Kg/s)

$\dot{m}_{f_{o_1}}$ = mass flow rate of potassium carbonate in Fuel cell-1 (Kg/s)

$\dot{m}_{f_{o_2}}$ = mass flow rate of potassium carbonate in Fuel cell-2(Kg/s)

$\dot{m}_{co_2_1}$ = mass flow rate of carbon dioxide in Fuel cell-1(Kg/s)

$\dot{m}_{co_2_2}$ = mass flow rate of carbon dioxide in Fuel cell-2(Kg/s)

$\dot{m}_{f_{he}}$ = mass flow rate of helium in the reheat and regenerative Braysson cycle (Kg/s)

p_b = Power output of Braysson cycle (KW)

p_f = Power output of Fuel cell (KW)

p_i = pressure at point i (Bar)

q_h = TΔS = (ΔH – ΔG) (KJ/Kg)

q_{h_1} =heat extracted from H₂O

q_{h_2} =heat extracted from CO₂

QH₁= heat supplied to reheat and regenerative braysson cycle from fuel cell -1

QH₂= heat supplied to reheat and regenerative braysson cycle from fuel cell -2

r_p = pressure ratio of main compressor

$$r_{p_1} = \left(\frac{p_4}{p_5}\right) = \left(\frac{p_6}{p_7}\right) = \sqrt{\frac{p_4}{p_7}} \quad r_{p_0} = \left(\frac{p_1}{p_9}\right)$$

$q_{i,p}$ = heat input to reheat and regenerative Braysson cycle (KW)

T_1 =inlet temperature of main compressor (K)

T_2 = inlet temperature of regenerator (K)

T_3 = outlet temperature of regenerator (K)

T_4 = turbine inlet temperature (K)

T_5 = high pressure turbine exit temperature (K)

T_6 = low pressure turbine inlet temperature (K)

T_7 = low pressure turbine outlet temperature (K)

T_8 = regenerator outlet temperature (K)

T_9 = cooler outlet temperature (K)

T_a = exit temperature after 1st stage of multi stage compressor (K)

T_2', T_5', T_7', T_a' are ideal temperatures (K)

v_i = volume at point i (m^3/Kg)

$w_{o,p}$ = work output of reheat and regenerative Braysson cycle (KW)

$w_{i,p}$ = work input to reheat and regenerative Braysson cycle (KW)

$w_{net,o}$ = overall net work of combined cycle = $p_b + p_{f_1} + p_{f_2}$ (KW)

η_c is efficiency of main compressor

η_t is efficiency of turbine

η_r is efficiency of regenerator

η_{1c} is efficiency of one-stage of multi stage compressor

$\eta_{b,c}$ = reheat and regenerative Braysson cycle efficiency

η_o = overall efficiency of the cycle (FC + reheat and regenerative Braysson cycle)

$\eta_{f,c}$ = fuel cell efficiency

γ = 1.667 for Helium (Adiabatic constant)

η_{exergy} = exergy efficiency of combined cycle

ΔH_1 = enthalpy change for H₂O (KJ/Kg)

ΔH_2 = enthalpy change for CO₂ (KJ/Kg)

ΔH = total enthalpy change in fuel cell (KJ/Kg)

ΔG_1 = Gibbs free energy change for H₂O (KJ/Kg)

ΔG_2 = Gibbs free energy change for CO₂ (KJ/Kg)

ΔG = Gibbs free energy change i.e. electric part of fuel cell output (KJ/Kg)

$T\Delta S$ = heat dissipated from fuel cell i.e. thermal part of fuel cell output (KJ/Kg)

TFC = total fuel consumption (Kg/hr)

SFC = specific fuel consumption (Kg/ KW-hr)

CHAPTER 1

1. INTRODUCTION

Thermodynamics plays a key role in the study of thermodynamic systems and devices that include transfer and transformation of energy. The word “thermodynamics” comes from Greek language “thermo” (heat) and “dynamics” (force) which basically means converting heat into work. All the activities in the nature involve interaction between energy and matter.

The science of energy (thermodynamics) presents a clear picture of interactions between energy and matter. All along our technological history, the development of sciences has enhanced our ability to harness energy and use it for society's needs. The increased awareness that the world's energy resources are limited has caused to re-examine the energy policies by countries and take drastic measures on waste and new techniques were developed for better utilization of the existing limited resources and that concept is known as Exergy.

The second law or exergy analysis offers a new insight into the true nature of losses in a thermal system which is generally overlooked by the first law analysis, also called energy analysis. The actual amount of energy that a source contains is estimated from energy analysis, which is generally of little value to build a power plant. The amount of energy that we can extract as a useful work from the source gives the work potential of that source which is of greater value known as Exergy. The concept of exergy and its importance is clearly understood from the study of the topics of energy & entropy. Energy, entropy and exergy concepts come from thermodynamics and are applicable to all fields of science and engineering.

1.1 Energy

The concept of energy was first introduced in mechanics by Newton when he hypothesized about kinetic and potential energies. However, the emergence of energy as a unifying concept in physics was not adopted until the middle of the 19th century and was considered one of the major scientific achievements in that century.

Energy is a scalar quantity that cannot be observed directly but can be recorded and evaluated by indirect measurements. Nature allows the conversion of work completely into heat, but heat is taxed when converted into work. Most of our daily activities and engineering applications involve energy transfer and energy change. The human body is a familiar example of biological system in which the chemical energy of the food or body fat is transformed into other forms of energy such as heat transfer and work transfer. Gas turbine engines commonly used for aircraft, propulsion, convert the chemical energy of the fuel into thermal energy that is used to run a gas turbine. Low temperature boiling fluids such as ammonia and refrigerant-134a absorb in the form of heat transfer, as they vaporize in the evaporator causing a cooling effect in the region being cooled. Therefore, a careful study of this topic is required to improve the design and performance of energy transfer systems.

1.2 Laws of Thermodynamics and their Significance

The science of thermodynamics is built primarily on three fundamental natural laws.

- The first law of thermodynamics state that "energy can change from one form to another but the total amount of energy remains constant" - law of conservation of energy.
- The second law of thermodynamics asserts that "energy has quality as well as quantity, and actual process occur in the direction of decreasing quality of energy"-law of degradation of energy.
- The third law states that "it is impossible by any procedure, no matter how idealised, to reduce any system to the absolute zero of temperature in a finite number of operations".

1.2.1. The first law of thermodynamics (FLT)

The First law of thermodynamics states that energy can be neither created nor destroyed; it just changes form. It defines internal energy as a state function and provides a formal statement of the conservation of energy. It provides no information about the ability of any thermodynamics process to convert heat into mechanical

work with full efficiency. The total energy E represents the sum of all forms of energy a system possesses, and the change in the energy content of a system during a process is expressed as ΔE_{system} . In the absence of electrical, magnetic, surface etc., effects the total energy in that case can be expressed as the sum of the internal, kinetic, and potential energies as

$$E = U + KE + PE \quad \text{and} \quad \Delta E_{\text{system}} = \Delta U + \Delta KE + \Delta PE$$

Energy can be transferred to or from a system in three forms: heat Q , work W , and mass flow m . Energy interactions are recognized at the system boundary as they cross it, and they represent the energy gained or lost by a system during a process. Then the FLT or energy balance for any system under going any kind of a process can be expressed as

$$E_{\text{in}} - E_{\text{out}} = \Delta E_{\text{system}}$$

That is, the net change (increase or decreases) in the total energy of the system during a process is equal to the difference between the total energy entering and the total energy leaving the system during that process.

The only two forms of energy interactions associated with a fixed mass or closed system are transfer and work. For a closed system undergoing a cycle, the initial and final states are identical and thus

$$\Delta E_{\text{system}} = E_2 - E_1 = E_{\text{out}}$$

Noting that a closed system does not involve any mass flow across its boundaries, the energy balance for a cycle can be expressed in terms of heat and work interactions as

$$W_{\text{net,out}} = Q_{\text{net,in}}$$

This is the network output during a cycle equal to net heat input for a cycle.

1.2.2. The second law of thermodynamics (SLT)

The first law of thermodynamics gives no information about direction; it merely states that when one form of energy is converted into other forms, an energy balance is maintained but it does not specify about the feasibility of the process. In this

regard, events could be vision that would not violate the FLT. e.g. transfer of a certain quantity of heat from low temperature body to a high temperature body, without expenditure of work. However, the reality shows that this is impossible and FLT becomes inadequate in picturing the complete energy transfer. Furthermore, experiments indicated that when energy in the form of heat is transferred to a system, only a portion of heat can be converted into work.

The SLT establishes the differences in quality between different forms of energy and explains why some processes can spontaneously occur. The second law of thermodynamics defines the fundamental physical quantity entropy as a randomized energy state unavailable for direct conversion to work. It also states that all spontaneous processes both physical and chemical proceed to maximize entropy, that is, to become more randomized and to convert energy into a less available form.

1.3. Exergy

Exergy also known as available energy is the maximum useful work that can be obtained from a system through a reversible process, when it is brought to a dead state. Exergy is a property which depends not only on the state of the system but also its surroundings. Hence, exergy is generally defined as the property of the composite system and surroundings. Since all the natural processes are irreversible in nature, exergy is destroyed during a process. The exergy destruction or the increase of entropy is a measure of the irreversibility of a natural process.

As already stated, exergy represents the useful form of work, it is customary to evaluate the exergy content of different forms of energy like heat energy, kinetic energy, potential energy, tidal energy, wind energy, geothermal energy, etc. Generally, since K.E and P.E can be completely converted into work ideally, the exergy quantum will be equal to the amount of K.E or P.E. However, with regards to heat energy, the quantum of exergy contained in a given heat energy depends on the temperature of the source of the heat. Like energy, exergy can be transferred or transported across the boundary of a system. For each type of energy transfer or transport there is a corresponding exergy transfer or transport.

1.3.1 Exergy analysis

Exergy analysis is a method that uses the conservation of mass and conservation of energy principles together with the SLT for the analysis, design and improvement of thermal systems. The exergy analysis forms the main part of modern thermodynamic approach in studying a thermal system. In general, more meaningful efficiency is evaluated with exergy analysis rather than energy analysis, since exergy efficiencies are always a measure of the approach to the ideal case. Engineers generally suggest that the thermodynamic performance of a process is best evaluated by performing an exergy analysis in addition to conventional energy analysis because exergy analysis appears to provide more insights and to be more useful in efficiency improvement efforts than energy analysis. It is important to highlight that exergy analysis can lead to a substantially reduced rate in the use of natural resources and the environment pollution by reducing the rate of discharge of waste products.

1.3.2 Energy balance for steady flow-system

Most devices encountered in practice are steady flow devices, such as turbines, heat exchangers, pumps, condensers, etc. Their mass, energy and entropy and volume remain constant during a steady flow process.

The steady flow energy equation represents the energy balance in a steady flow process. It is given by the expression,

$$h_1 + \frac{C_1^2}{2} + gz_1 + q_{1-2} = h_2 + \frac{C_2^2}{2} + gz_2 + W_s$$

Applying the steady flow energy equation to the turbine while neglecting potential energy and kinetic energy and assuming that the process is isentropic then

$$h_1 = h_2 + W_s$$

$$W_s = h_1 - h_2$$

Similarly, by applying steady flow energy equation to a pump while neglecting potential energy and kinetic energy and assuming that the process is isentropic, we have

$$h_2 = h_1 + W_s$$

$$W_s = h_2 - h_1$$

1.4 Second Law Efficiency (or) Exergy Efficiency

A common measure on energy used efficiency is the first law efficiency. The first law efficiency is defined as the ratio of the output energy of a device to the input energy of device. The first law is concerned only with the quantities of energy, and disregards the forms in which the energy exists. It does not also discriminate between the energies available at different temperatures. It is the second law of thermodynamics which provides a means of assigning a quality index to energy. The concept of available energy or exergy provides a useful measure of energy quality.

With this concept, it is possible to analyse means of minimizing the consumption of available energy to perform a given process, thereby ensuring the most efficient possible conversion of energy for the required task.

The second law efficiency of a process is defined as the ratio of the minimum available energy or exergy which must be consumed to do a task divided by the actual amount of energy consumed in performing the task.

$$\eta_{II} = \frac{\text{minimum exergy intake to perform the given task}}{\text{actual exergy intake to perform the same task}}$$

This definition is specifically used for devices like turbines, pumps etc which either produce or consume shaft work.

The second law efficiency can also be defined as the ratio of exergy recovered from a system to the exergy supplied. This definition holds for devices like heat exchangers, boilers, condensers etc.

$$\eta_{II} = \frac{\text{Energy Recovered}}{\text{Energy Supplied}}$$

1.5 Fuel cell:

A fuel cell is an electro chemical cell that converts the potential energy from a fuel into electricity through an electrochemical reaction of hydrogen fuel with oxygen or another oxidizing agent. Fuel cells are different from batteries in requiring a continuous source of fuel and oxygen (usually from air) to sustain the chemical reaction, whereas in a battery the chemical energy comes from chemicals already present in the battery. Fuel cells can produce electricity continuously for as long as fuel and oxygen are supplied.

There are many types of fuel cells, but they all consist of an anode, a cathode, and an electrolyte that allows positively charged hydrogen ions (protons) to move between the two sides of the fuel cell. At the anode a catalyst causes the fuel to undergo oxidation reactions that generate protons (positively charged hydrogen ions) and electrons. The protons flow from the anode to the cathode through the electrolyte after the reaction. At the same time, electrons are drawn from the anode to the cathode through an external circuit, producing direct current electricity. At the cathode, another catalyst causes hydrogen ions, electrons, and oxygen to react, forming water.

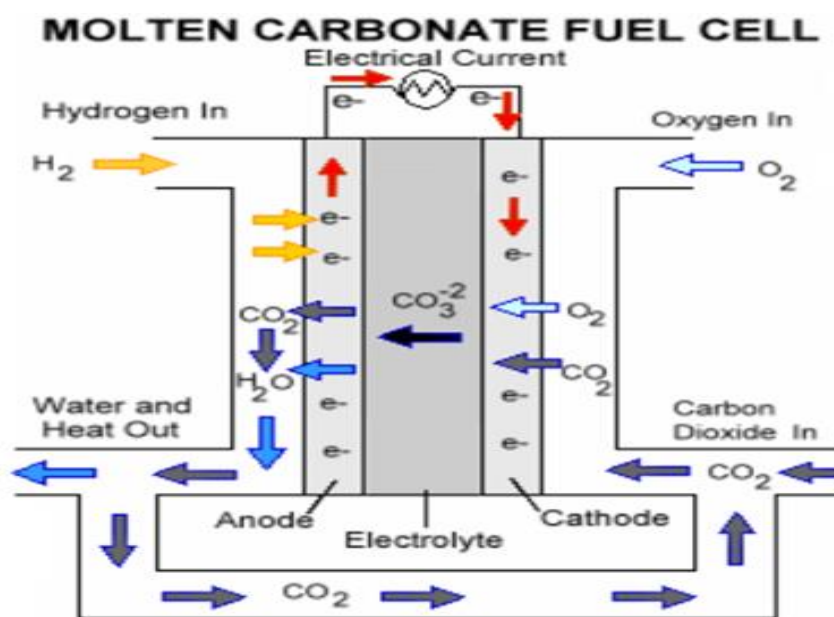


Fig 1.1 Molten Carbonate Fuel Cell (MCFC)

1.5.1 History:

The origin of fuel cell technology is credited to Sir William Robert Grove (1811-1896). Grove developed an improved wet-cell battery in 1838 which brought him fame. Using his research and knowledge that electrolysis used electricity to split water into hydrogen and oxygen he concluded that the opposite reaction must be capable of producing electricity. Using this hypothesis, Grove developed a device which would combine hydrogen and oxygen to produce electricity. Grove had developed the world's first gas battery. It was this gas battery which has become known as the fuel cell.

Ludwig Mond (1839-1909) along with assistant Carl Langer conducted experiments with a hydrogen fuel cell that produced 6 amps per square foot at 0.73 volts.

It was Friedrich Wilhelm Ostwald (1853-1932), the founder of the field of physical chemistry, who experimentally determined the relationship between the different components of the fuel cell, including the electrodes, electrolyte, oxidizing and reducing agent, anions and cations. Ostwald's work opened doors into the area of fuel cell research by supplying information to future fuel cell researchers.

During the first half of the twentieth century, Emil Baur (1873-1944) conducted extensive research into the area of high temperature fuel cell devices which used molten silver as the electrolyte. His work was performed along with students at Braunschweig and Zurich.

Francis Thomas Bacon (1904-1992) performed research and significant developments with high pressure fuel cells. Bacon was successful in developing a fuel cell that used nickel gauze electrodes and operated at pressures up to 3000 psi.

1.5.2 Types:

Fuel cells come in many varieties; however, they all work in the same general manner. They are made up of three adjacent segments: the anode, the electrolyte, and the cathode. Two chemical reactions occur at the interfaces of the three different segments. The net result of the two reactions is that fuel is consumed, water or carbon dioxide is created, and an electric current is created, which can be used to power electrical devices, normally referred to as the load.

At the anode a catalyst oxidizes the fuel, usually hydrogen, turning the fuel into a positively charged ion and a negatively charged electron. The electrolyte is a substance specifically designed so ions can pass through it, but the electrons cannot.

The freed electrons travel through a wire creating the electric current. The ions travel through the electrolyte to the cathode. Once reaching the cathode, the ions are reunited with the electrons and the two react with a third chemical, usually oxygen, to create water or carbon dioxide.

Fuel cells are classified by the type of electrolyte they use and by the difference in startup time ranging from 1 second for proton exchange membrane fuel cells (PEMFC) to 10 minutes for molten carbonate fuel cells (MCFC) and solid oxide fuel cells (SOFC). A related technology is flow batteries, in which the fuel can be regenerated by recharging. Individual fuel cells produce relatively small electrical potentials, about 0.7 volts, so cells are "stacked", or placed in series, to create sufficient voltage to meet an application's requirements. In addition to electricity, fuel cells produce water, heat and, depending on the fuel source, very small amounts of nitrogen dioxide and other emissions. The energy efficiency of a fuel cell is generally between 40–60%; however, if waste heat is captured in a cogeneration scheme, efficiencies up to 85% can be obtained.

Types of fuel cell include:

Fuel cells can be classified in several ways.

1. Based on the type of electrolyte :(i) Phosphoric Acid Fuel cell (PAFC)(ii) Alkaline Fuel Cell (AFC)(iii) Solid Polymer Fuel Cell (SPFC)(iv) Molten Carbonate Fuel Cell (MCFC)(v) Solid Oxide Fuel Cell (SOFC)
2. Based on types of the fuel and oxidant :(i) Hydrogen – Oxygen Fuel Cell (ii) Hydrogen – Air Fuel Cell (iii) Ammonia – Air Fuel Cell(iv) Hydrocarbon – Air Fuel Cell
3. Based on operating temperature: (i) Low temperature fuel cell (below 150 degrees) (ii) Medium temperature fuel cell (150-250 degrees) (iii) High temperature fuel cell (250-800 degrees) (iv) Very high temperature fuel cell (800-1100 degrees)
4. Based on application :(i) Fuel cell for space applications(ii) Fuel cell for vehicle propulsion(iii) Fuel cell for submarines(iv) Fuel cell for defense applications(v) Fuel cell for commercial applications
5. Based on chemical nature of electrolyte :(i) Acidic electrolyte type(ii) Alkaline electrolyte type(iii) Neutral electrolyte type

1.5.3 Applications:

1. The first commercial use of fuel cells came more than a century later in NASA space programs to generate power for satellites and space capsules.
2. Since then, fuel cells have been used in many other applications.
3. Fuel cells are used for primary and backup power for commercial, industrial and residential buildings and in remote or inaccessible areas.
4. They are also used to power fuel cell vehicles, including forklifts, automobiles, buses, boats, motorcycles and submarines.

1.5.4 Advantages and Disadvantages of Fuel Cells:

Advantages:

1. High operating pressure which results in lower irreversibilities.
2. High operating temperature which results in improved reaction kinetics and lower irreversibilities.
3. High efficiency.
4. Suitable for use as combined cycle.
5. Ability to work with many hydrocarbons such as natural gas.

Disadvantages:

1. High costs.
2. Not suitable for portable applications.
3. Sealing.
4. Cell component degradation at high operating temperature.
5. Corrosive electrolyte results in the anode and cathode performance degradation.

1.6 Evolution of Braysson Cycle

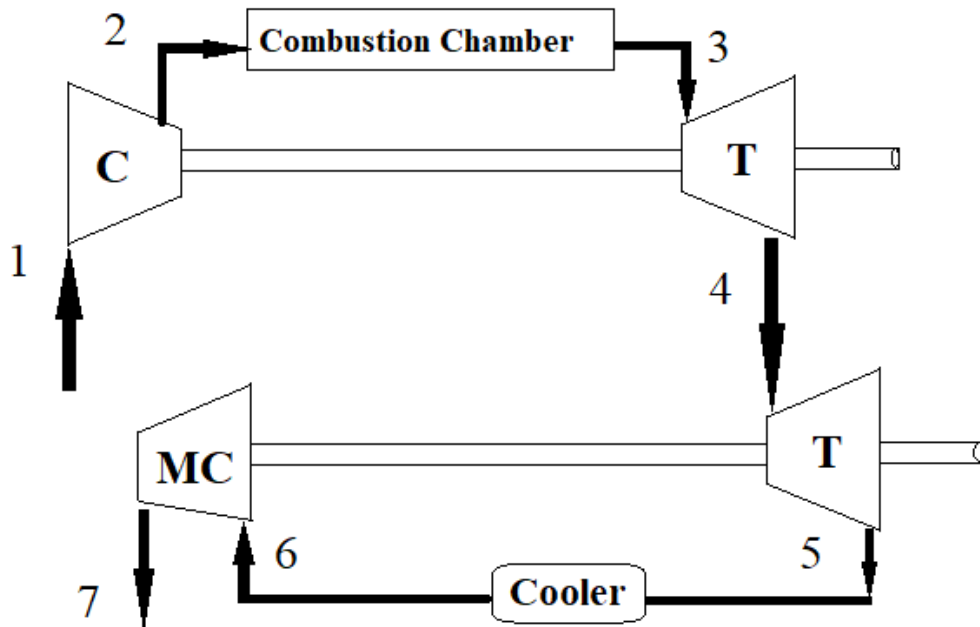


Fig 1.2 Layout of Braysson cycle with cooler and multi stage compressor

A power generation cycle has highest efficiency when it runs on reversible cycle with isothermal heat addition and low temperature isothermal heat rejection. The temperature of heat rejection can be decreased by implementing a combined cycle power plant in which heat rejected from Brayton cycle is used to drive the steam turbine cycle. Such cycles are being used in the world due to their higher energy and exergy efficiencies.

In 1997 T H Frost first proposed an alternative to the combined cycles and termed it as Braysson cycle. The Braysson cycle is inherently an air driven cycle and therefore the complexities of a combined cycle plant are totally eliminated in this cycle.

Later in 2015 reheat regenerative Braysson cycle was proposed, its efficiency was observed to be almost equal to ideal Braysson cycle.

Braysson is a hybrid of high temperature heat addition Brayton cycle and the low temperature heat rejection Ericsson cycle. It incorporates the advantages of both the cycles.

1.6.1 Brayton cycle:

Gas turbines are described thermodynamically by the Brayton cycle, in which air is compressed isentropically, combustion occurs at constant pressure, expansion occurs isentropically and heat is rejected isobarically to the ambient. Its components are:

- Compressor
- Combustion chamber
- Turbine
- Heat Exchanger

Process:

- Isentropic compression process: Ambient air is drawn into the compressor.
- Isobaric heat addition process: The compressed air then runs through a combustion chamber, where fuel is burned, heating that air at constant-pressure process.
- Isentropic expansion process: The heated air is expanded through the turbine. Some of the work extracted by the turbine is used to drive the compressor.
- Isobaric heat rejection process : Heat rejected to atmosphere.

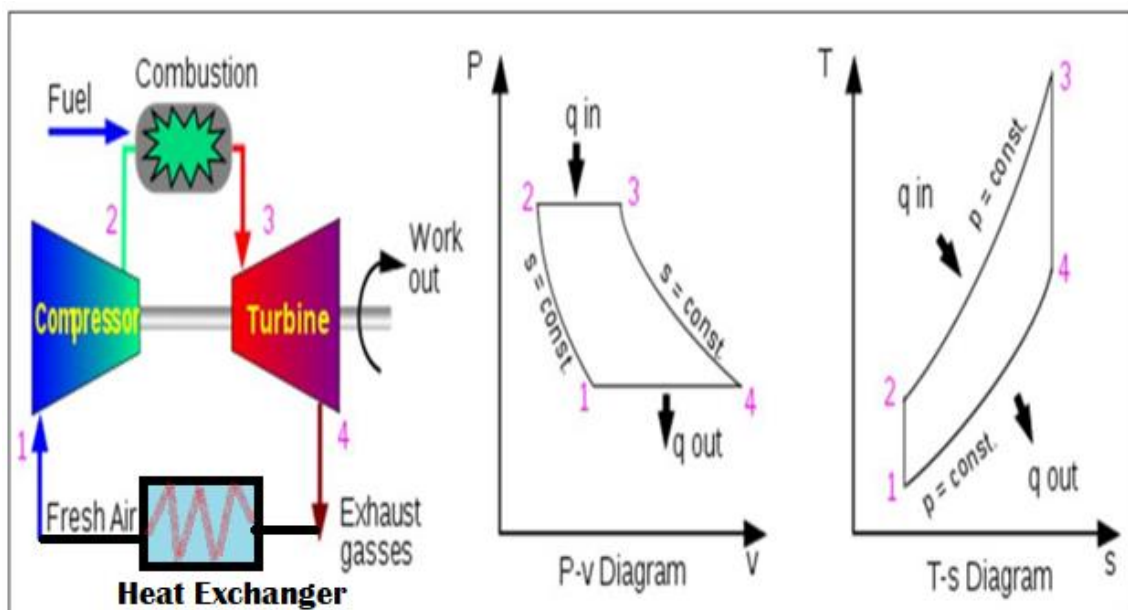


Fig 1.3 Layout of a Brayton cycle with P-V & T-S plot

1.6.2 Ericsson cycle:

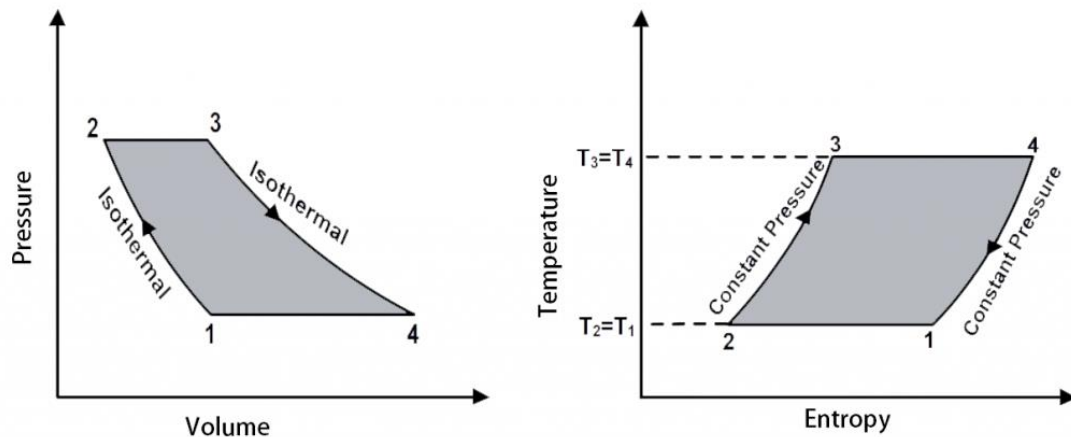


Fig 1.4 P-V & T-S plot for an Ericsson cycle

The Ericsson cycle consists of two isothermal and two constant pressure processes.

- Process1-2: Reversible Isothermal compression.
- Process2-3: Isobaric heat addition.
- Process3-4: Reversible Isothermal expansion.
- Process4-1: Isobaric heat rejection.

The heat addition and rejection take place isothermally. The net effect is that the heat need to be added only at constant temperature $T_3=T_4$ and rejected at the constant temperature $T_1=T_2$. The advantage of the Ericsson cycle over the Carnot and Sterling cycles is its smaller pressure ratio for a given ratio of maximum to minimum specific volume with higher mean effective pressure.

The thermal efficiency of Ericsson cycle is given by

$$\eta_{th} = \frac{T_H - T_L}{T_H} = 1 - \frac{T_L}{T_H}$$

The Ericsson cycle does not find practical application in piston engines but is approached by a gas turbine employing a large number of stages with heat exchangers, insulators and reheaters.

1.6.3 Concept of ideal cycle:

Ideal Braysson cycle, also known as reversible cycle is a hybrid cycle consists of a gas turbine coupled with a bottoming turbine (Ericsson cycle) where the working fluid expands to attain ambient temperature thereby expanding to vacuum pressure(0.04bar) The bottoming turbine is coupled with multi stage intercooled compressor for isothermal heat rejection. All the processes in the cycle are reversible and thus the second law efficiency of individual components is obtained as 100%. The exergy losses are considered in the combustion chamber as the heat addition takes place at finite temperature difference.

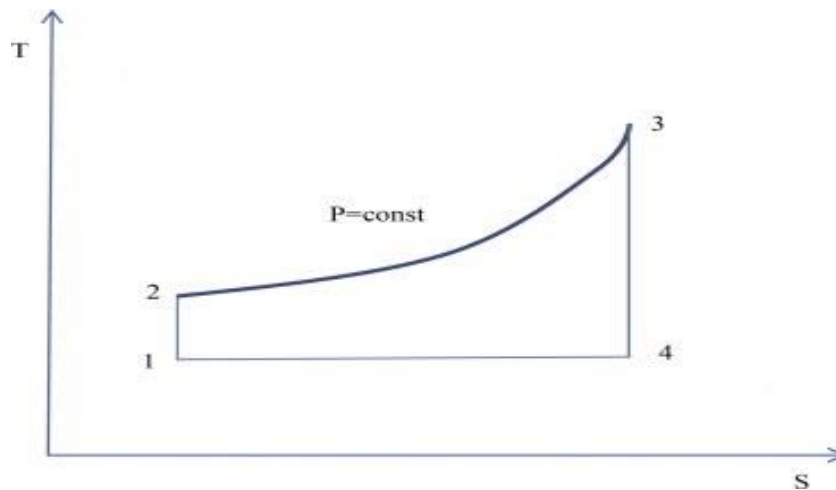


Fig 1.5 T-S plot for an ideal Braysson cycle.

- Process1-2: Reversible Isentropic compression.
- Process2-3: Isobaric heat addition.
- Process3-4: Reversible Isentropic expansion.
- Process4-1: Isothermal heat rejection.

1.7 Reheat & Regenerative Braysson Cycle

1.7.1 Regeneration:

The Process during which heat is transferred to a thermal energy storage device, during one part of the cycle and is transferred back to the working fluid during another part of the cycle. The high pressure air leaving the compressor can be heated by transferring heat to it from the hot exhaust gases in a counter flow heat exchanger, which is also known as a regenerator or a recuperator.

1.7.2 System description:

A schematic diagram of Braysson cycle with regeneration and reheating is shown in fig 1.6. The cycle consists of a compressor, combustion chamber, main gas turbine, reheater, regenerator, reheat gas turbine, cooler and a multistage compressor. Both the main turbine and the reheat gas turbine are mechanically coupled to electric generators and compressors. The gases at the exit of the main turbine are reheated to the maximum temperature of the cycle before being passed into the reheat turbine where they further expand to sub-atmospheric pressure.

The regenerator improves the cycle efficiency by utilizing the waste heat of the gases on the downstream of reheat turbine. The gases exiting the regenerator are cooled further before letting them into the multistage compressor. The gases are then pressurized to atmospheric pressure in the multi stage compressor and exited to the ambient.

For the purpose of reheating, we have to use another fuel cell for the temperature requirement. From the calculations, The temperature rise in reheater and normal heating are almost similar. Hence we can use the same fuel cell with same specifications for reheating also.

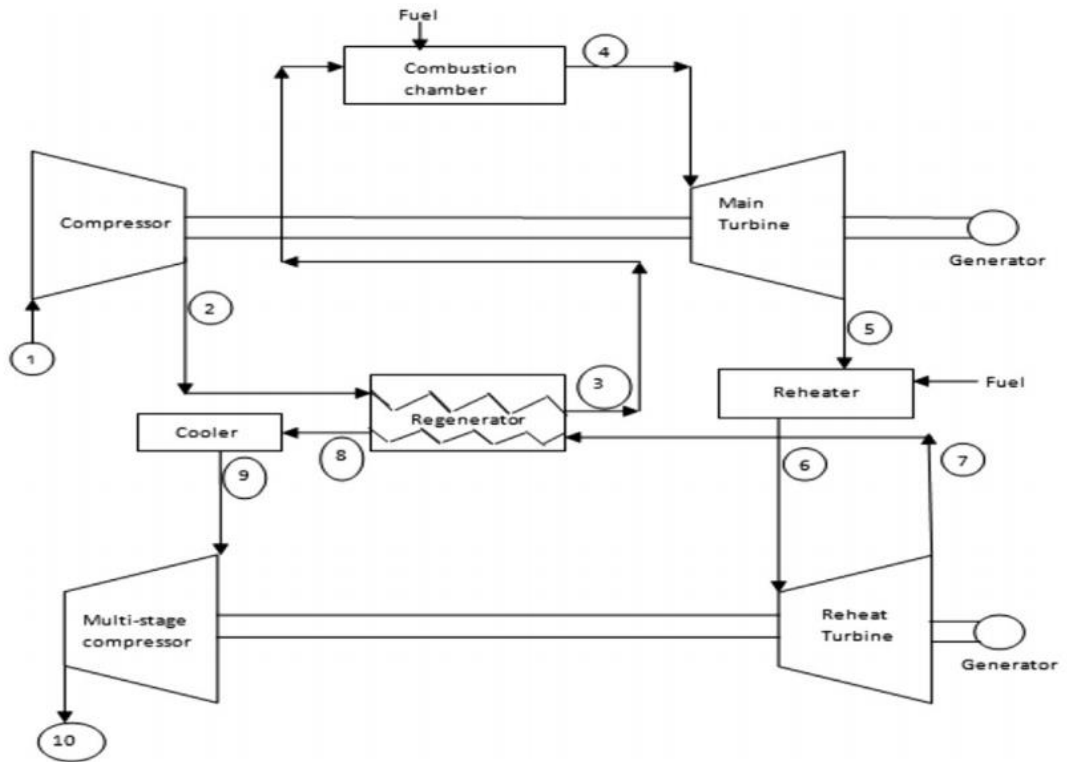
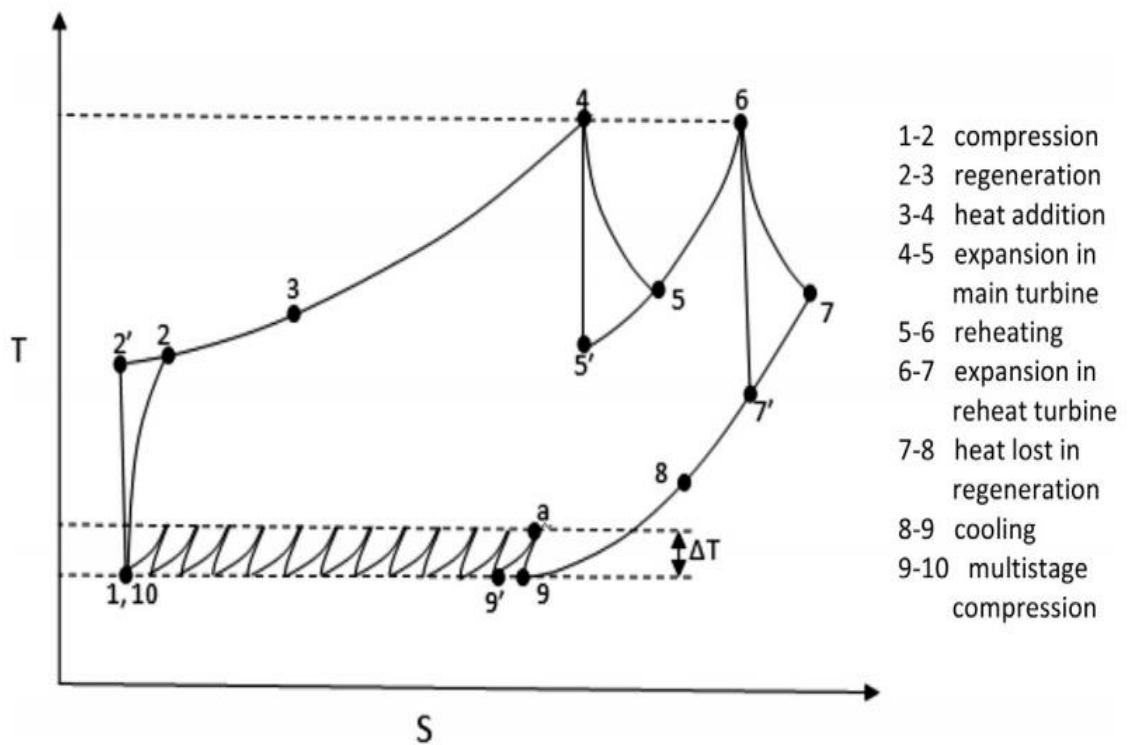


Fig 1.6. Schematic diagram of Braysson cycle with reheat and regeneration

and

T-S diagram for Reheat & Regenerative Braysson cycle



1.7.2.1 Polytropic expansion (1-2):

The compression process is accomplished using a compressor that is coupled to the primary turbine. The process is assumed to be polytropic process and the efficiency of the compressor is taken as 80%. However it is assumed that there are no heat losses to the surroundings. The compressor pressurizes the gas from ambient pressure to the required pressures. The ratio of output pressure to the input pressure of the compressor is taken as pressure ratio of the system (r_p).

1.7.2.2 Regeneration (2-3):

In Regenerator, the high pressure air leaving the compressor is heated by transferring heat to it from the hot exhaust gases coming from the secondary turbine. This Process occurs at constant pressure. Then the compressed air at high temperature enters the combustion chamber.

1.7.2.3 Isobaric heat addition (3-4):

The heat addition process takes place at constant pressure in the heat exchanger by transferring heat from the fuel cell to the working fluid of the Braysson cycle (helium)

1.7.2.4 Polytropic expansion (4-5) & (6-7):

The expansion of working fluid takes place in the main and reheats gas turbines with intermediate reheat. The intermediate pressure at which reheating is carried out is optimized for maximum work output of the turbines. The downstream pressure of reheat turbine is considered as vacuum pressure

1.7.2.5 Isobaric heat addition in Reheater (5-6):

The work output of a turbine operating between two pressure levels can be increased by expanding the gas in stages and reheating it in between, (i.e.) utilizing multistage expansion with reheating. The heat transfer from the fuel cell to the air takes place in the reheater at constant pressure to increase the working fluid temperature to the maximum temperature of the cycle.

1.7.2.6 Regeneration at constant pressure (7-8):

The exchange of heat takes place between hot gases coming from the turbine and the compressed air obtained from the compressor. The hot gases transfer their heat to the compressed air and come out at lower temperature and then enter the cooler. This process occurs at constant pressure.

1.7.2.7 Isobaric heat rejection (8-9):

This Process is done using cooler for further decreasing of the temperature of the hot gases, thereby decreasing the compressor work. There are no pressure changes during the process.

1.7.2.8 Isothermal heat rejection (9-10):

The isothermal heat rejection is achieved with the help of a multistage intercooled compressor which is powered by the bottoming turbine. The heat rejection and compression takes place simultaneously in the multi-stage intercooled compressor. The compression is considered as isentropic process and the heat rejection take place at constant pressure in every stage. The optimum number of stages is taken as 4 from the thermodynamic considerations. The pressure increases from vacuum pressure to ambient pressure. The intercooling is achieved by using hollow stators as suggested by Frost et.al. However, the temperature drop per stage should be limited to around 10°C to maintain nearly isothermal conditions. Since the additional power required to drive this unit is drawn from a bottoming turbine the net work output remains almost same when compared with a conventional Brayton cycle based gas turbine operating under the same conditions. The heat is rejected to a low temperature sink (atmosphere).

CHAPTER 2

2. LITERATURE REVIEW

Mehdi Mehrpooya et al. [1] introduced Fuel cell, Stirling engine and absorption chiller hybrid system. Molten carbonate Fuel cell exhausted heat is used as heat source of the Stirling engine. Overall and electrical efficiencies of the hybrid system are 71.71% and 42.28%.

Frost et al. [2] proposed an alternative to the combined cycles and termed it as Braysson cycle. The Braysson cycle is inherently an air driven cycle, and therefore the complexities involved in installing and running the heat recovery steam generator, condenser and other auxiliaries of a combined cycle plant are totally eliminated in this cycle. Braysson cycle is a hybrid of the high temperature heat addition Brayton cycle and the low temperature heat rejection Ericsson cycle. The Braysson cycle was subjected to further studies based on both the first and the second law analysis by many researchers.

R.Chandramouli. et al.[3]

Energy and exergy based thermodynamic analysis of reheat and regenerative Braysson cycle the conventional Braysson cycle has not found practical use due to the difficulty in achieving isothermal compression. To make its implementation a reality, the original cycle has been modified by incorporating regenerator and a cooler before the final compression process. Reheating was included for augmenting the power output. Expressions for exergy efficiency and exergy destruction for all the components are derived along with the energy and exergy efficiencies of the complete cycle.

Zheng et al. [4] carried out an exergy analysis for an irreversible Braysson cycle and analysed the influence of various parameters on its performance. It has been shown that both the power output and the efficiency of the cycle are greater than those of Brayton cycle.

Zheng et al. [5] also derived the analytical formula for power output, efficiency, maximum power output and the corresponding efficiency of an endo-reversible Braysson cycle with the heat resistance losses in the hot and cold-side heat exchangers using finite time thermodynamics. He also analysed the influence of the design parameters on the performance of the cycle.

Sreenivas et al. [6] performed the second law analysis of an irreversible Braysson cycle. The overall second law efficiency and the component-wise second law efficiencies were derived. The thermodynamic losses occurring in each component were obtained.

Liqiang Duan et al. [7] proposed a novel pressurized MCFC hybrid system with CO₂ capture. The effects of the key parameters on new system performances are studied. The economic performance analyses of the new system are made. The efficiency penalty of the new system is only 0.91% after capturing 90% CO₂. The economic performance of new system should be further improved.

Akbar Saheli et al. [8] performed the 3E analyses of a CHP plant based on biomass gasifier and MCFC. The waste heat of the biomass-fueled MCFC system is recovered by HRSG, Stirling engine, and ORC. The system yields an exergy efficiency of 50.18% with a CO₂ emission of 0.289 t/MWh. The gasifier and fuel cell have the highest rates of exergy destruction.

Md. Alizadeh Jarchlouei et al. [9] has modeled Molten carbonate fuel cell using Lagrange method of undetermined multipliers. With Lagrange method, the analysis of the MCFC stack can be done more easily. A mathematical model is developed in the EES software. Methane is used as a fuel for molten carbonate fuel cell stack. Steam reforming is performed for methane. A simulation of a MCFC stack performance by the Lagrange method at a specified state, results in an efficiency of 50.3% & output power of 554.3 kW.

Yasin et al. [10] performed the analysis of endo-reversible Braysson cycle based on ecological criteria. The ecological objective function was defined and its maximization was achieved for various design parameters.

S. Campanari et al. [11] performed an analysis of the application of Molten Carbonate Fuel Cells (MCFC) in a natural gas fired combined cycle power plant to capture CO₂ from the exhaust of the gas turbine. The gas turbine flue gases are used as cathode feeding for a MCFC, where CO₂ is transferred from the cathode to anode side, concentrating the CO₂ in the anode exhaust. This stream is then sent to a CO₂ removal section consisting either in (i) an oxygen combustion of residual fuel compounds, or (ii) a cryogenic CO₂ removal section, cooling the exhaust stream in the heat recovery steam generator.

S. Campanari et al. [12]

The MCFC is based on Ansaldo Fuel Cells experience, fed with natural gas processed by an external reformer which is thermally integrated within the FC module. Differently from more conventional approaches to CO₂ capture, it works increasing the plant power output, acting as an active CO₂ concentrator. The plant shows the potential to achieve a CO₂ avoided ranging between 58 and 68%, depending on the configuration while taking advantage from the introduction of the fuel cell, the final electric efficiency is lower from 0.2 to 0.8 points lower than the original combined cycle (57.8% LHV in the most efficient configuration). The power output increases by about 22%, giving a potentially relevant advantage with respect to competitive carbon capture technologies. Molten Carbonate Fuel Cells (MCFCs) are the only fuel cells which may work as CO₂ concentrators/separators, if fed by the exhaust gases of a power plant.

Junlin Zheng et al. [13] Exergy analysis for a Braysson cycle.

An exergy analysis has been carried out for an irreversible Braysson cycle. The analytical formulae of power output and exergy efficiency are derived. The influences of various parameters on the exergy performance are analyzed by numerical calculation, and the results obtained have been compared with those of Brayton cycle under the same conditions. It is shown that the exergy loss in the combustion is the largest in the Braysson cycle, and both specific work and exergy efficiency of the cycle are larger than those of Brayton cycle.

Umberto Desideri et al. [14] investigated the chemical composition of flue gases from existing cogeneration plants, in order to perform a feasibility study of the MCFC technology for CO₂ separation. For this purpose, a model of a MCFC using as input the exhaust gas of a combined heat and power plant has been developed. A capture system is modeled with molten carbonate fuel cells based on measured flue gas composition and analyzed. Carbon capture is highly efficient with MCFC.

Alireza Haghghat Mamaghani et al. [15] proposed a novel hybrid system, integrating high temperature MCFC-GT (molten carbonate fuel cell-gas turbine) and ORC (organic Rankine cycle), which provides the possibility to achieve high electrical and exergetic efficiencies owing to the subsequent electrical power output in the bottoming cycle. After developing a mathematical model, comprehensive energetic, exergetic, economic and environmental evaluations (4E analysis) are performed and a multi-objective optimization method is utilized to find optimal solutions while considering the exergetic and economic objectives simultaneously. Two conflicting objectives including total exergetic efficiency and total cost rate of the system in multi-objective optimization are taken into account to build a set of Pareto optimal solutions. This optimum solution results in the exergetic efficiencies of 35.6%, 44.3%, and 54.9% for the fuel cell system, ORC cycle and the whole hybrid system respectively. The study reveals that introducing the ORC bottoming cycle leads to about 5% improvement in the exergetic efficiency of the proposed plant.

Mehdi Mehrpooya et al. [16] developed and examined a pioneer hybrid system consisted of MCFC, Gas Turbine, steam cycle, and Thermo Photo Voltaic system. A TPV system together with a steam cycle was included for heat recovery. Incorporating the TPV system increased the proposed hybrid system efficiency by about 2.5%. Incorporating the GT to the MCFC enhanced the system's efficiency to 54.83%. The efficiency of the proposed hybrid system was found to be 67.3%.

Nanotechnology used for manufacturing of fuel cell compartments, such as the anode, has improved the performance of MCFCs in recent times [17]. Introducing the new micro-composite electrodes might increase the durability, conductivity and most importantly, the life time of the electrodes during fuel cell operation.

Commercialization of MCFC systems in the current competitive market, where the material and design innovation are much easier to be achieved for other types of fuel cells, requires a thorough understanding of the new technology and it emerges as a wide area of research to be completed [18].

Zhang et al. [19] presented a novel model of the solar-driven thermodynamic cycle system consisting of a solar collector and a Braysson heat engine. The performance characteristics of the system were optimized on the basis of the linear heat-loss model of solar collector and the irreversible cycle model of a Braysson heat engine. The main drawback of Braysson cycle is the difficulty in achieving isothermal compression in multistage intercooled compressor. However, a few proposals were made by some researchers.

Georgiou et al. [20] also proposed a multistep intercooled compression process on a solar-driven Braysson heat engine as feasible solution for implementing isothermal compression in Braysson cycle. The results indicated that such a plant may reach efficiency levels of above 30%, i.e. exceeding the efficiencies of the conventional Photovoltaic plants by a wide margin.

Chandramouli et al. [21] have recently proposed reheat and regenerative Braysson cycle with the inclusion of cooler and showed that it reaches the efficiency of the conventional Braysson cycle at a very lower pressure ratio. The study also included the influence of number of stages of multistage intercooled compressor on exergy efficiency and came to the conclusion that it can work with fewer stages ($N = 10$) and attain higher efficiency than the conventional Braysson cycle with isothermal compression (which is an ideal proposition). Thus, one needs not go for isothermal compression. Hence a parametric analysis of this reheat and regenerative Braysson cycle is required to study the effect of different parameters on the cycle performance for its practical implementation.

SCOPE OF THE LITREATURE WORK

Direct energy conversion systems plays an important role in energy conversion from one form to other form, and there are many direct energy conversion systems but in those fuel cells are more applicable to use in mobile applications and many other. These fuel cells work under certain temperature range, out of all MCFC can run under high temperature range so we choose these fuel cells to reuse the waste heat. We have decided to combine this fuel cell with thermodynamic cycle, by studying the above literature work we have opted for a certain thermodynamic cycle and also the cathode, anode and electrolyte of MCFC fuel cell.

The above literature contains an information about suitable materials for MCFC to run it at high efficiency. They mentioned that MCFC have a capability to run on various hydrocarbon fuels but the main drawback is that carbon deposition happens on anode part of MCFC due to this after some time the work output decreases. These papers also provide various techniques to overcome that and also how to improve the efficiency of MCFC by reforming process. This also contains information about combined Brayton and Ericsson cycle which is known as Braysson cycle having high efficiency but it has no practical applications to overcome that the paper [3] provides information about reheat and regeneration Braysson cycle can be considered.

By studying the above literature work we have concluded and decided to reuse the waste heat of MCFC by combing it with Reheat and Regenerative Braysson cycle to improve its efficiency and performed thermodynamic analysis.

CHAPTER 3

3. THERMODYNAMIC ANALYSIS

3.1 SYSTEM DESCRIPTION

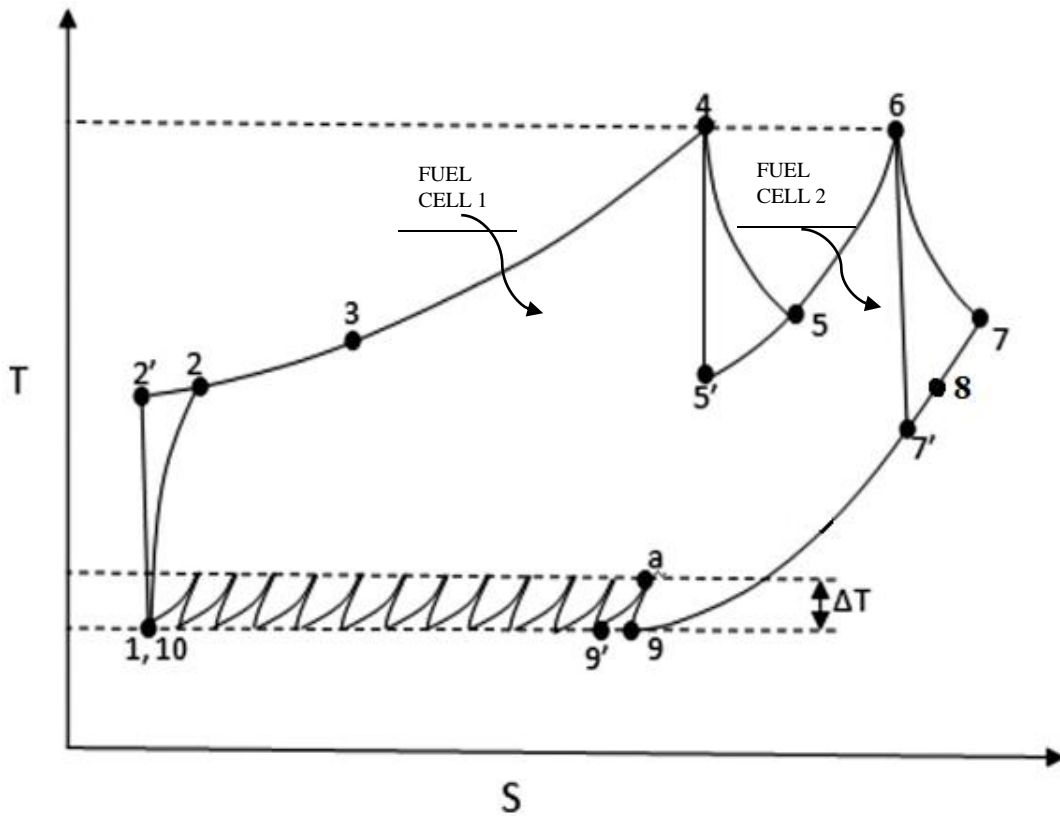


Fig 3.1 T-S diagram for Reheat & Regenerative Braysson cycle

The T-S plot of the Thermodynamic cycle is represented described below.

1. Isentropic compression (1-2)
2. Regeneration (2-3) & (7-8)
3. Isobaric heat addition (3-4)
4. Isentropic expansion (4-5) & (6-7)
5. Isobaric heat addition in reheater (5-6)
6. Isobaric heat rejection (8-9)
7. Isothermal heat rejection using multi stage compressor (9-1)

3.2 Energy analysis:

3.2.1 Isentropic compression (1-2)

The temperature of the air after compression can be calculated using the following equation

$$\begin{aligned}
 p_1 v_1^\gamma &= p_2 v_2^\gamma \\
 p_1 \left(\frac{T_1}{p_1}\right)^\gamma &= p_2 \left(\frac{T_2'}{p_2}\right)^\gamma \\
 (p_1)^{1-\gamma} * (T_1)^\gamma &= (p_2)^{1-\gamma} * (T_2')^\gamma \\
 \left(\frac{T_2'}{T_1}\right) &= (r_p)^{\frac{\gamma-1}{\gamma}} \\
 \eta_c &= \frac{T_2' - T_1}{T_2 - T_1} \\
 T_2 &= T_1 + \frac{T_1 * \left(r_p^{\frac{\gamma-1}{\gamma}} - 1\right)}{\eta_c} \dots\dots\dots (1)
 \end{aligned}$$

3.2.2 Isentropic expansion (4-5)

The temperature at the outlet of high pressure turbine can be calculated by using following equation

$$\begin{aligned}
 p_4 * v_4^\gamma &= p_5 * v_5^\gamma \\
 \left(\frac{T_5'}{T_4}\right) &= \left(\frac{p_5}{p_4}\right)^{\frac{\gamma-1}{\gamma}} = \left(\frac{1}{r_{p1}}\right)^{\frac{\gamma-1}{\gamma}} = r_{p1}^{\left(\frac{1-\gamma}{\gamma}\right)} \\
 \eta_t &= \frac{T_4 - T_5}{T_4 - T_5'} \\
 T_5 &= T_4 + \eta_t (T_5' - T_4) \\
 T_5 &= T_4 + \eta_t \left(r_{p1}^{\frac{1-\gamma}{\gamma}} - 1\right) \dots\dots\dots (2)
 \end{aligned}$$

The temperature at the end of reheat process is observed as same temperature at inlet of high pressure turbine.

$$T_6 = T_4 \dots\dots\dots (3)$$

Note:

Regeneration will be possible only if $T_5 > T_2$

When the gas expands through the reheat turbine the same temperature are observed as in case of expansion through the main turbine.

$$T_7 = T_5 \dots\dots\dots (4)$$

3.2.3 Regeneration (2-3) & (7-8)

The temperature at the end of regeneration process can be calculated by using the following equation

$$\eta_r = \frac{T_3 - T_2}{T_7 - T_2}$$

$$T_3 = \eta_r * (T_7 - T_2) + T_2 \dots\dots\dots (5)$$

The temperature at the end of regeneration process can be calculated by following equation

$$T_8 = T_7 - T_3 + T_2 \dots\dots\dots (6)$$

The temperature at the end of the isobaric heat rejection is same as the input temperature of the cycle

$$T_9 = T_1 \dots\dots\dots (7)$$

3.2.4 Isothermal heat rejection using multi stage compressor (9-1)

The temperature at the end of multi stage intercooled compressor can be determined by the following equation

$$\frac{T_a'}{T_9} = r_{pi}^{\frac{\gamma-1}{\gamma}}$$

$$\eta_{1c} = \frac{T_a' - T_9}{T_a - T_9}$$

$$T_a = T_9 + \frac{(r_{po}^{\frac{\gamma-1}{\gamma}} - 1)}{\eta_{1c}} \dots\dots\dots (8)$$

Work output of Braysson cycle can be obtained by

$$w_{o,p} = c_p * (T_4 - T_5) + c_p * (T_6 - T_7)$$

Work input to Braysson cycle is obtained by

$$w_{i,p} = c_p * (T_2 - T_1) + n (c_p(T_a - T_9))$$

Heat input to Braysson cycle is obtained by

$$q_{i,p} = q_{h1} * (\dot{m}_{h2o1} + \dot{m}_{h2o2}) + q_{h2} * (\dot{m}_{co21} + \dot{m}_{co22})$$

Where,

m_{f_1} and m_{f_2} are mass flow rates of water in fuel cells 1 and 2 respectively

Braysson cycle efficiency is obtained by

$$\eta_{b.c} = \frac{w_{o,p} \text{ of braysson} - w_{i,p} \text{ of braysson}}{q_{i,p}}$$

Overall efficiency is obtained by

$$\eta_o = \frac{p_b + p_{f_1} + p_{f_2}}{\Delta H_o}$$

Fuel cell efficiency is given by

$$\eta_{f.c} = \frac{\Delta G}{\Delta H} \dots\dots\dots (9)$$

Where,

$$\Delta H_o = \Delta H1 * (\dot{m}_{h2o1} + \dot{m}_{h2o2}) + \Delta H2 * (\dot{m}_{co21} + \dot{m}_{co22})$$

$$p_b = w_{o,p} \text{ of Braysson} - w_{i,p} \text{ of Braysson}$$

$$p_{f_1} = (\dot{m}_{h2o1} * \Delta G1) + (\dot{m}_{co21} * \Delta G2)1$$

$$p_{f_2} = (\dot{m}_{h2o2} * \Delta G1) + (\dot{m}_{co22} * \Delta G2)$$

$$q_h = (\Delta H - \Delta G)$$

Mass flow rate of H₂O can be obtained from the equation

$$\dot{m}_{f_{he}} * c_p * (T_4 - T_3) = \dot{m}_{f_1} * Q_h \dots\dots\dots (10)$$

$$\dot{m}_{f_{he}} * c_p * (T_6 - T_5) = \dot{m}_{f_2} * Q_h \dots\dots\dots (11)$$

Mass flow rate of methane in fuel cell 1, $\dot{m}_{f_1} = \frac{16}{44} * (\dot{m}_{co21})$

Mass flow rate of methane in fuel cell 2, $\dot{m}_{f_2} = \frac{16}{44} * (\dot{m}_{co22})$

$$\text{Mass flow rate of water in fuel cell , } \dot{m}_{h2o1} = \frac{9}{11} * (\dot{m}_{co21})$$

$$\text{Mass flow rate of water in fuel cell , } \dot{m}_{h2o2} = \frac{9}{11} * (\dot{m}_{co22})$$

$$\text{TFC} = (\dot{m}_{f1} + \dot{m}_{f2}) * 3600$$

$$\text{SFC} = \frac{\text{TFC}}{W_{net_o}}$$

Where ,

$$W_{net_o} = p_b + p_{f1} + p_{f2}$$

3.3 Exergy analysis:

Rate of exergy supplied = Rate of exergy recovered + Rate of exergy destroyed

Therefore,

$$\text{Rate of exergy destroyed} = \text{Rate of exergy supplied} - \text{Rate of exergy recovered} \dots (12)$$

$$\text{Exergy efficiency} = \frac{\text{Rate of exergy recovered}}{\text{Rate of exergy supplied}} \dots (13)$$

3.3.1 Isentropic compression (1-2)

$$\text{Rate of exergy supplied} = c_p * (T_2 - T_1)$$

$$= c_p * \frac{T_1 * \left(r_p^{\frac{\gamma-1}{\gamma}} - 1 \right)}{\eta_c} \dots (14)$$

$$\text{Rate of exergy recovered} = c_p * (T_2 - T_1) - T_0 * (s_2 - s_1)$$

$$= c_p \frac{T_1 \left(r_p^{\frac{\gamma-1}{\gamma}} - 1 \right)}{\eta_c} - T_0 c_p \left(\ln \left(\frac{T_2}{T_1} \right) - \left(\frac{\gamma-1}{\gamma} \right) \ln(r_p) \right) \dots (15)$$

3.3.2 Regeneration (2-3) & (7-8)

$$\eta_e = \frac{e_3 - e_2}{e_7 - e_8}$$

$$= \frac{(h_3 - T_0 s_3) - (h_2 - T_0 s_2)}{(h_7 - T_0 s_7) - (h_8 - T_0 s_8)}$$

$$= \frac{c_p(T_3 - T_2) - T_0(s_3 - s_2)}{c_p(T_7 - T_8) - T_0(s_7 - s_8)}$$

$$= \frac{c_p(T_3 - T_2) - T_0 c_p \ln\left(\frac{T_3}{T_2}\right)}{c_p(T_7 - T_8) - T_0 c_p \ln\left(\frac{T_7}{T_8}\right)} \dots \dots \dots (16)$$

$$\text{Rate of exergy destroyed} = c_p \left[(T_7 - T_8) - T_0 \ln\left(\frac{T_7}{T_8}\right) \right] - c_p \left[(T_3 - T_2) - T_0 \ln\left(\frac{T_3}{T_2}\right) \right]$$

$$\dots \dots \dots (17)$$

3.3.3 Fuel Cells 1 and 2

Chemical Exergy supplied CH₄, $ces_{CH_4} = 51756$ KJ/Kg of methane

Chemical Exergy supplied K₂CO₃, $ceo = 123.3$ KJ/Kg of Potassium carbonate

$$\text{Exergy recovered from Fuel cell 1} = (((m_{h_2o1} * ((q_{h1}) * (1 - (T_0/T)) + \Delta G_1))) + (m_{co21} * (q_{h2} * (1 - (T_0/T)) + \Delta G_2))) / ((m_{f_{CH_4}} * ces_{CH_4}) + (m_{f_{O_2}} * ces_o)) \dots \dots (18)$$

$$\text{Exergy supplied to fuel cell 1} = (\dot{m}_{f_1} * ces_{CH_4}) + (\dot{m}_{f_{O_2}} * ces_o) \dots \dots (19)$$

$$\text{Exergy recovered from Fuel cell 2} = (((m_{h_2o2} * ((q_{h1}) * (1 - (T_0/T)) + \Delta G_1))) + (m_{co22} * (q_{h2} * (1 - (T_0/T)) + \Delta G_2))) / ((m_{f_{CH_4}} * ces_{CH_4}) + (m_{f_{O_2}} * ces_o)) \dots \dots (20)$$

$$\text{Exergy supplied to fuel cell 2} = (\dot{m}_{f_2} * ces_{CH_4}) + (\dot{m}_{f_{O_2}} * ces_o) \dots \dots (21)$$

3.3.4 Heating of fluid (3-4) & (5-6)

$$\text{Exergy recovered (3-4)} = C_{ph} * ((T_4 - T_3) - T_0 * (\log(T_4/T_3))) \dots \dots (22)$$

$$\text{Exergy supplied (3-4)} = (m_{h_2o1} * (q_{h1}) * (1 - (T_0/T)) + m_{co21} * (q_{h2}) * (1 - (T_0/T))) \dots (23)$$

$$\text{Exergy recovered (5-6)} = C_{ph} * ((T_6 - T_5) - T_0 * (\log(T_6/T_5))) \dots \dots (24)$$

$$\text{Exergy supplied (5-6)} = (m_{h_2o2} * (q_{h1}) * (1 - (T_0/T)) + m_{co22} * (q_{h2}) * (1 - (T_0/T))) \dots (25)$$

3.3.5 Isentropic expansion (4-5), (6-7)

$$\text{Rate of exergy supplied} = c_p(T_4 - T_5) - c_p T_0 \left[\ln \left(\frac{T_4}{T_5} \right) - \left(\frac{\gamma-1}{\gamma} \right) \ln r_{p1} \right] \dots \dots \dots (26)$$

$$\text{Rate of exergy recovered} = c_p(T_4 - T_5) \dots \dots \dots (27)$$

3.3.6 Cooler (8-9)

$$\text{Exergy recovered} = 0 \dots \dots \dots (28)$$

$$\text{Exergy supplied} = c_p * (T_8 - T_9) - c_p * T_0 * \ln \left(\frac{T_8}{T_9} \right) \dots \dots \dots (29)$$

3.3.7 Multistage compressor (9-a-1)

$$\begin{aligned} \text{Exergy recovered in compressor} &= N * c_p * T_9 * \left(\frac{r_{p0}^{\left(\frac{\gamma-1}{\gamma N}\right)-1}}{\eta_{1c}} \right) + N c_p * T_0 * \\ &\left(\ln \left(1 + \frac{r_{p0}^{\left(\frac{\gamma-1}{\gamma N}\right)-1}}{\eta_{1c}} \right) \right) + N c_p * T_0 * \frac{(\gamma-1)(\ln r_{p0})}{\gamma N} \dots \dots \dots (30) \end{aligned}$$

$$\begin{aligned} \text{Exergy recovered in Intercooler} &= (N - 1) c_p * (T_a - T_9) - (N - 1) * c_p * T_0 * \\ &\ln \left(1 + \frac{r_{p0}^{\left(\frac{\gamma-1}{\gamma N}\right)-1}}{\eta_{1c}} \right) \dots \dots \dots (31) \end{aligned}$$

Total exergy recovered in multi stage compressor system, = eq(30) – eq(31)

3.3.8 Exergy efficiency of combined system (Braysson cycle + fuel cell)

η_{exergy}

$$\begin{aligned} &= \frac{p_b + p_{f1} + p_{f2}}{\left((\dot{m}_{f_{H_1}} + \dot{m}_{f_{H_2}}) * \text{chemical exergy of } H_2 \right) + \left((\dot{m}_{f_{O_1}} + \dot{m}_{f_{O_2}}) * \text{chemical exergy of } O_2 \right)} \\ &= 1 - \frac{\text{overall destroyed}}{\text{supplied}} \end{aligned}$$

CHAPTER 4

4. RESULTS AND DISCUSSIONS

Waste heat recovery from an ideal Molten Carbonate Fuel Cell using a Reheat and Regenerative Braysson cycle is analysed in this work. The following assumptions have been considered in the analysis. The number of stages in the multistage compressor is fixed at 4, the back pressure of low-pressure turbine is fixed to 0.4 Bar and the turbines, compressors & regenerator efficiencies are assumed as 80%. It is also assumed that only 80% of waste heat liberated from the fuel cell is utilized for running the reheat and regenerative Braysson cycle and the effectiveness of regenerator is 1. It has been assumed that there are no pressure drops of the working fluid in the system. The analysis has been performed considering helium as working fluid. From the expressions developed, the exergy efficiency and exergy destruction of each device is obtained. The overall energy and exergy efficiencies of the cycle are also evaluated. The chemical exergies of methane and potassium carbonate are 51810.7 KJ/ and 612.82 KJ/Kg respectively.

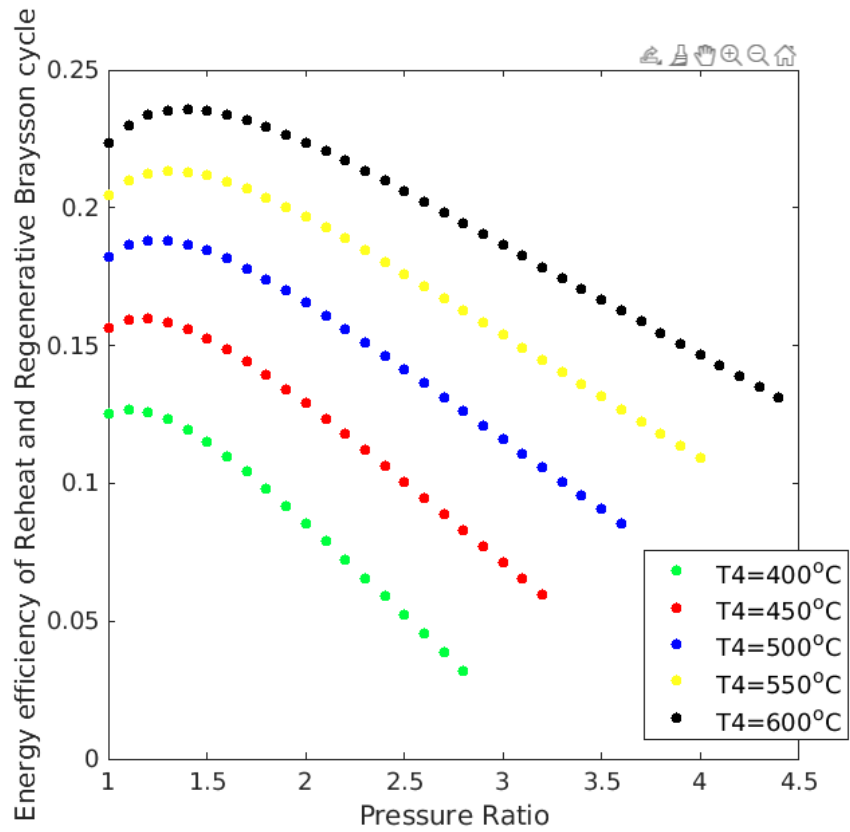


Fig 4.1 Energy efficiency of Reheat and Regenerative Braysson cycle vs. Pressure ratio at different TIT

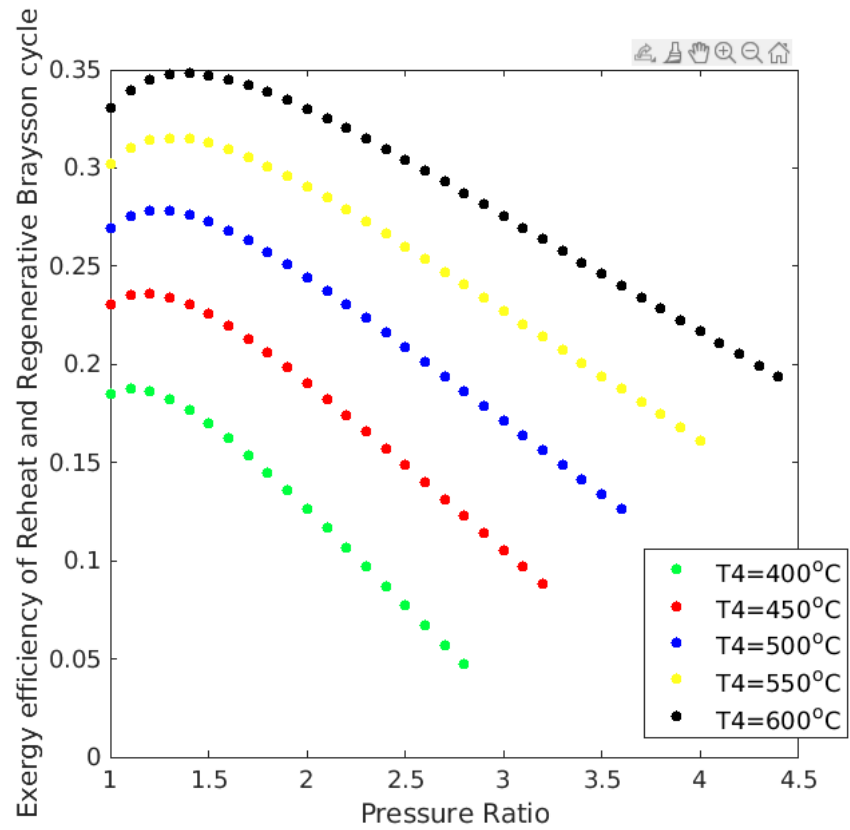


Fig 4.2 Exergy efficiency of Reheat and Regenerative Braysson cycle vs. Pressure ratio at different TIT

It has been observed that there is a limiting pressure ratio, when regeneration is adopted. Though regeneration increases the thermal efficiency of the cycle, it imposes a limit on the maximum pressure ratio in the cycle. Pressure ratios higher than the limiting value would mean that the temperature of compressed air exceeds the temperature of gases at the exit of reheat turbine. In such eventuality, regeneration becomes impracticable. This can be observed from the figure 1.6.

As T_4 increases, corresponding value of limiting pressure ratio also increases. The reason for this is as T_4 increases the exit temperature of reheat turbine, T_7 also increases. So, the limiting condition for regeneration i.e $T_7 > T_2$ is satisfied for higher pressure ratios also. Therefore, as the value of T_4 increases, corresponding value of limiting pressure ratio also increases.

Also, both the efficiencies increase abruptly with pressure ratio up to the optimum value, and thereafter decline gradually with further rise in pressure ratio as shown in the figures 4.1 and 4.2. For lesser pressure ratio, the work output of the turbines is minimal, though regeneration is effective and reduces the heat input from the external source. Therefore efficiencies increase up to an optimum value. At higher pressure ratios above the optimum value, the influence of regeneration diminishes, thereby lessening the cycle efficiency. It is because at higher pressure ratios T_2 increases. Also, T_7 decreases. So, the difference, $(T_7 - T_2)$ decreases. Hence, the range of regeneration, $(T_3 - T_2)$ decreases with increase in pressure ratio i.e regeneration becomes less effective.

As T_4 increases, both the energy and exergy efficiencies of the regenerative and reheat Braysson cycle increase. This is due to the fact that as T_4 (Turbine inlet temperature) increases, turbine gives more work output, as the gases expands over a higher range of temperatures.

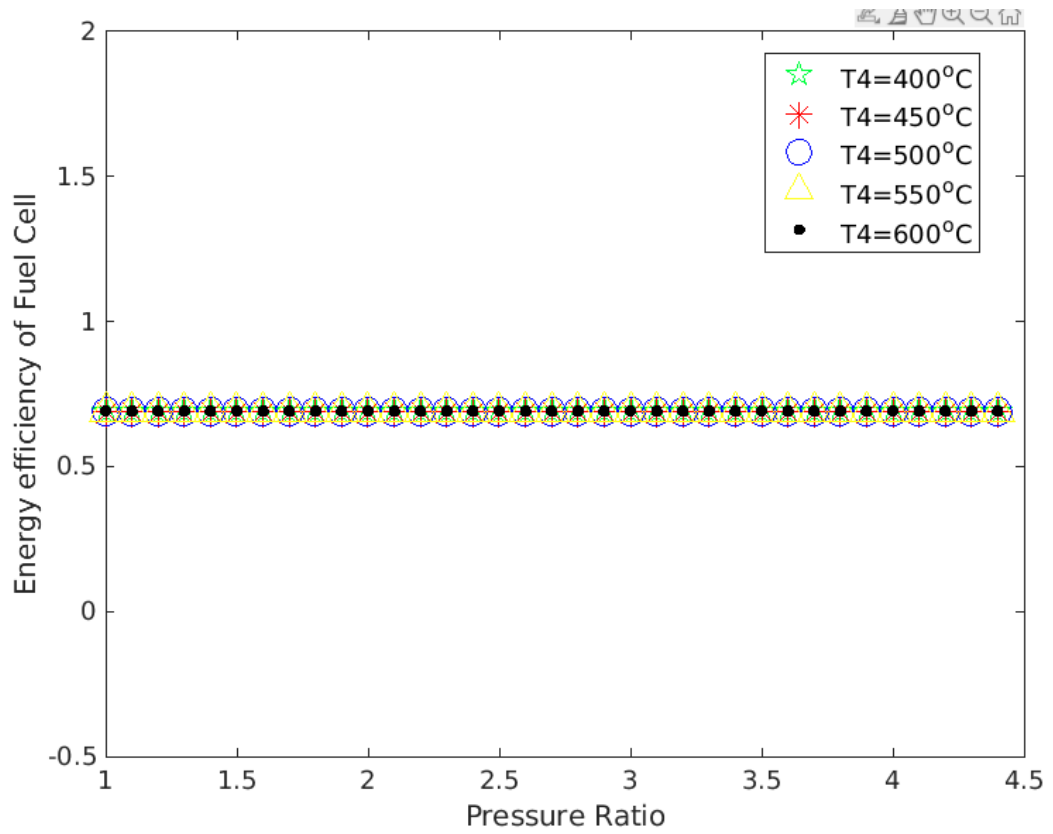


Fig 4.3 Energy efficiency of Fuel Cell vs. Pressure Ratio for different TIT

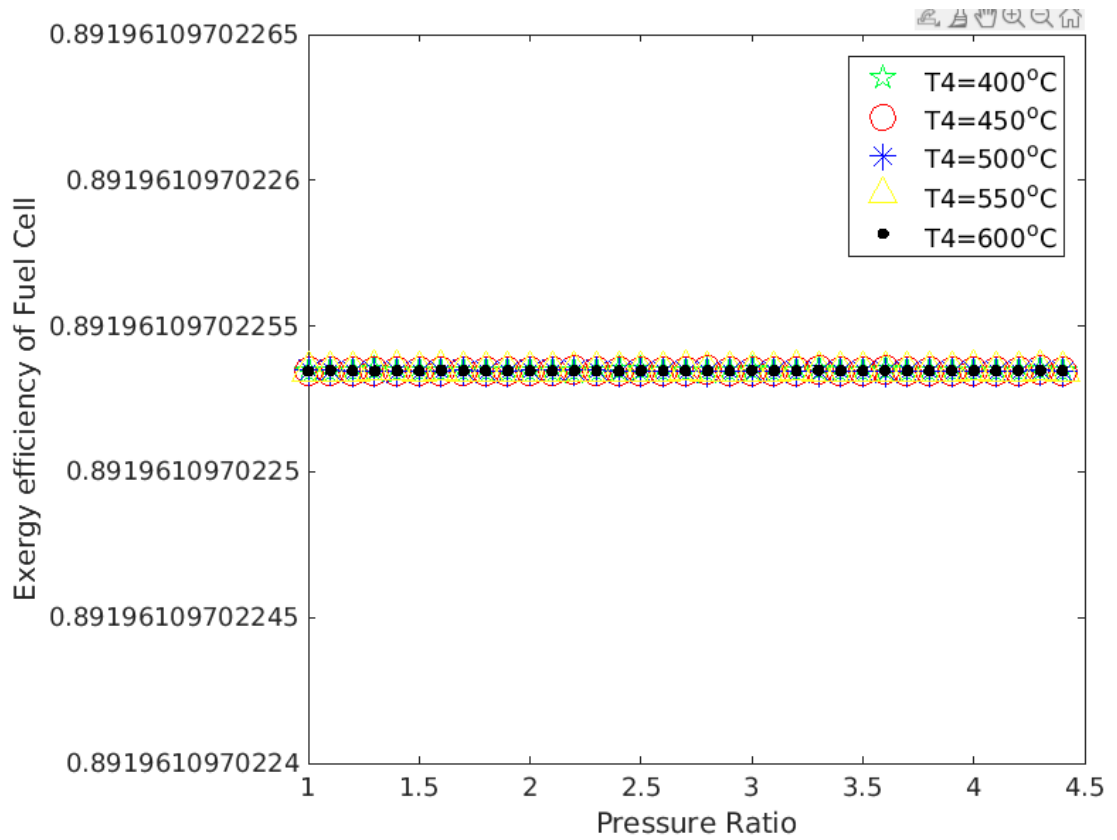


Fig 4.4 Exergy efficiency of Fuel Cell vs. Pressure Ratio for different TIT

Both the energy and exergy efficiencies of fuel cell are independent of pressure ratio as shown in the fig 4.3 & 4.4 since these terms are independent of mass flow rate of water in the fuel cell as shown in equations (9), (13), (18), (19).

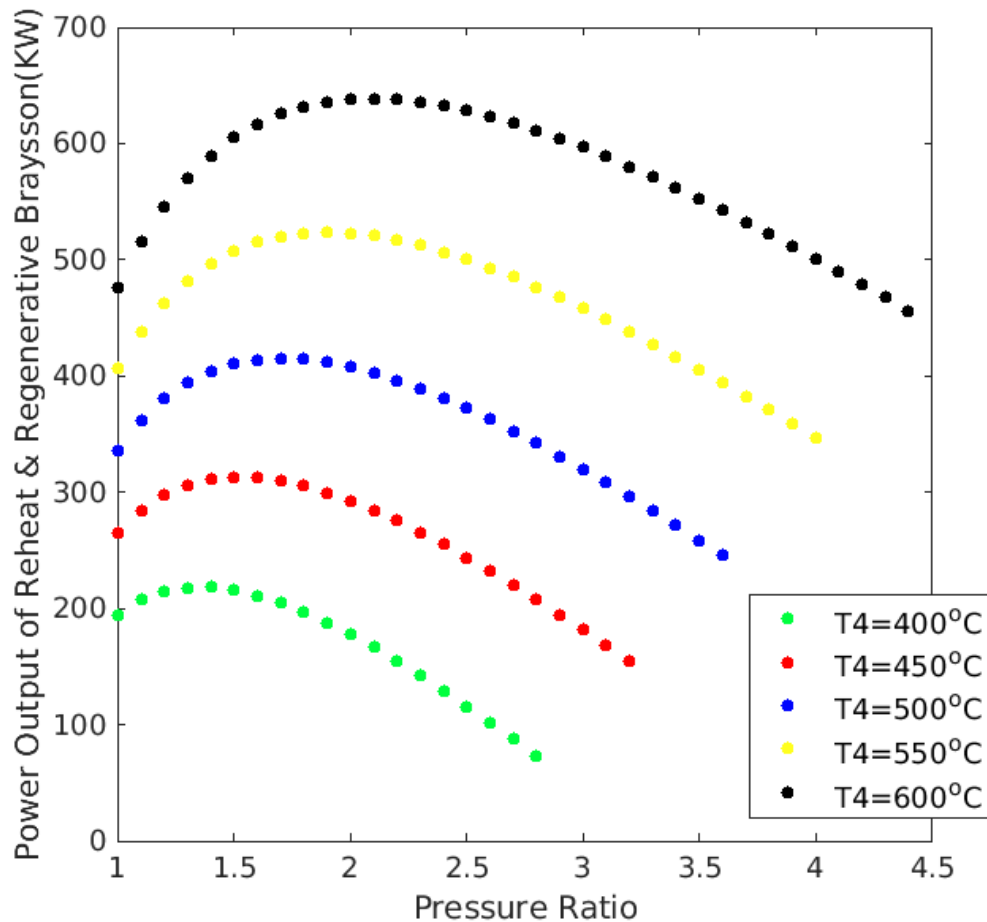


Fig 4.5 Power Output of Reheat & Regenerative Braysson Cycle vs. Pressure Ratio for different TIT

It can be observed from the figure 4.5 that as the pressure ratio increases power output from the Braysson cycle increases initially and then decreases, this is due to the fact that as the pressure ratio increases work output from turbines increase but at the same time, compressor work input is also increasing. Therefore, net power output from the Braysson cycle increases with pressure ration till an optimum value and then decreases. As T_4 increases, work output of turbines increases and hence net power output increases with increasing T_4 .

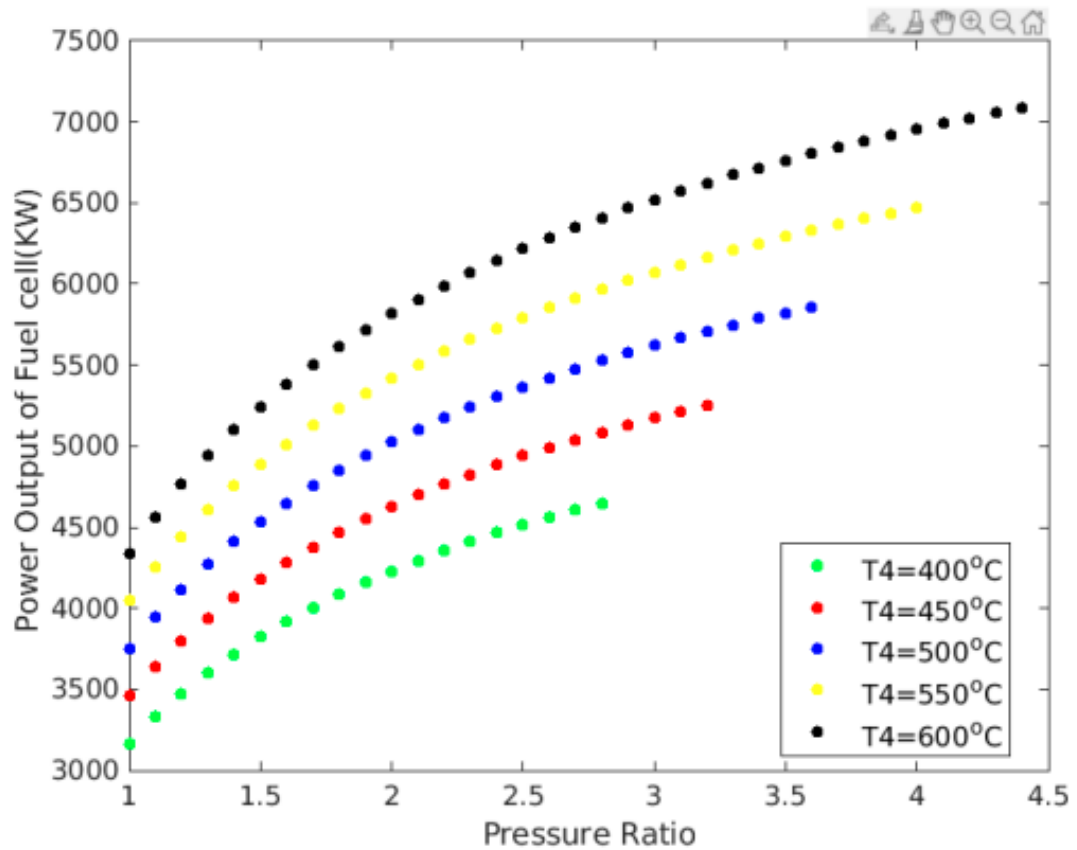


Fig 4.6 Power Output of Fuel Cell vs. Pressure Ratio for different TIT

It can be seen from the figure 4.6 that power output of fuel cell increases with increase in T_4 and with increase in pressure ratio.

As T_4 increases, the difference, $(T_4 - T_3)$ increases and hence more heat is to be supplied to the Braysson cycle. Hence, the mass flow rate of water in the fuel cell must be more (eq10) and hence power output of fuel cell also increases.

Also, as pressure ratio increases, power output of fuel cell increases. This is because as mentioned already in fig. 4.1 and 4.2, as pressure ratio increases, T_3 value decreases as regenerator becomes less effective. So, the difference $(T_4 - T_3)$ increases and thereby more heat is to supplied from the fuel cell. Hence, the mass flow rate increases there by increasing the power output of fuel cell.

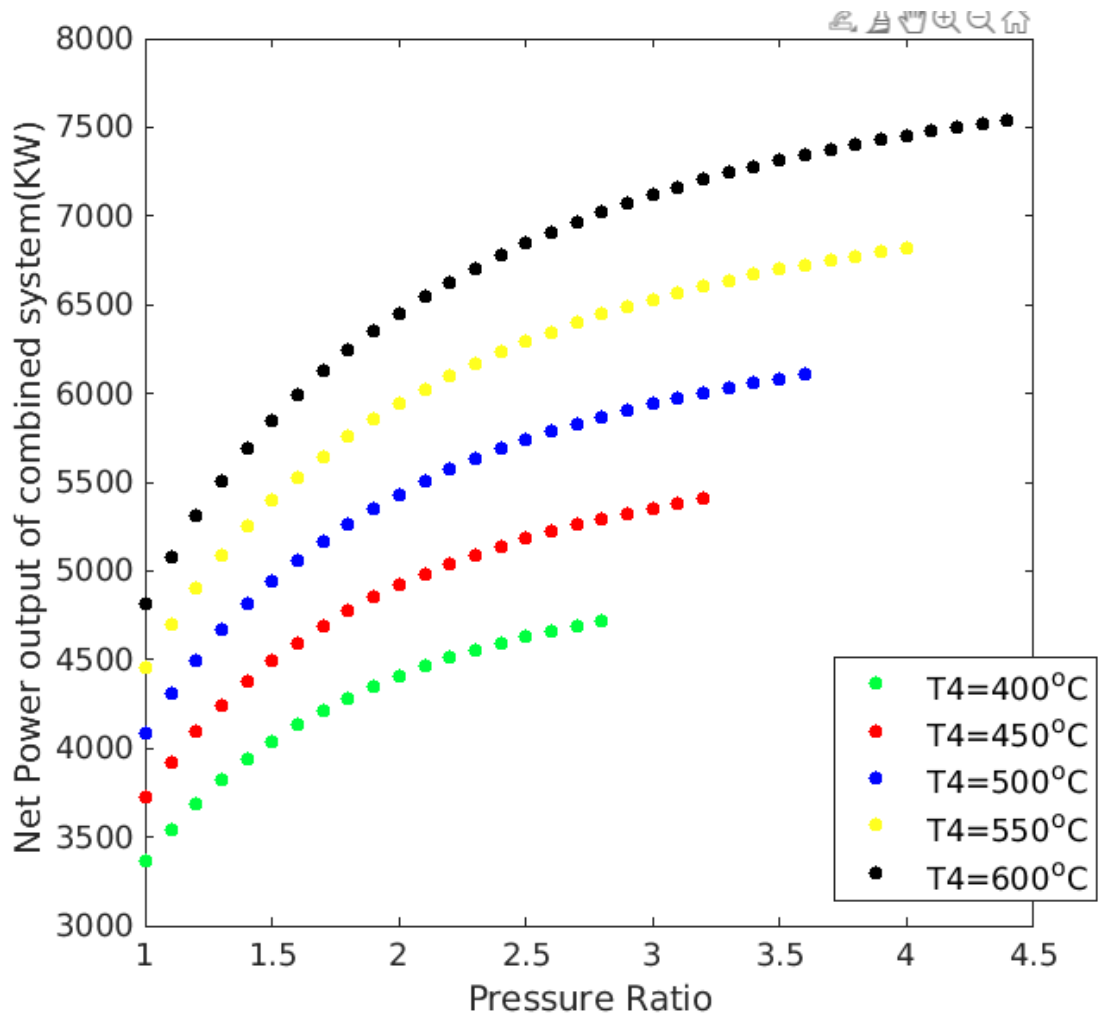


Fig 4.7 Net power output of combined system (KW) vs Pressure ratio for different TIT

The net power output of combined cycle increases with pressure ratio and TIT. Also, there does not exist an optimum pressure ratio because the effect of fuel cell is dominating (which showed increasing trend as given in fig-4.6) when compared to the Braysson cycle power output (which showed increasing and decreasing trend as given in fig- 4.5).

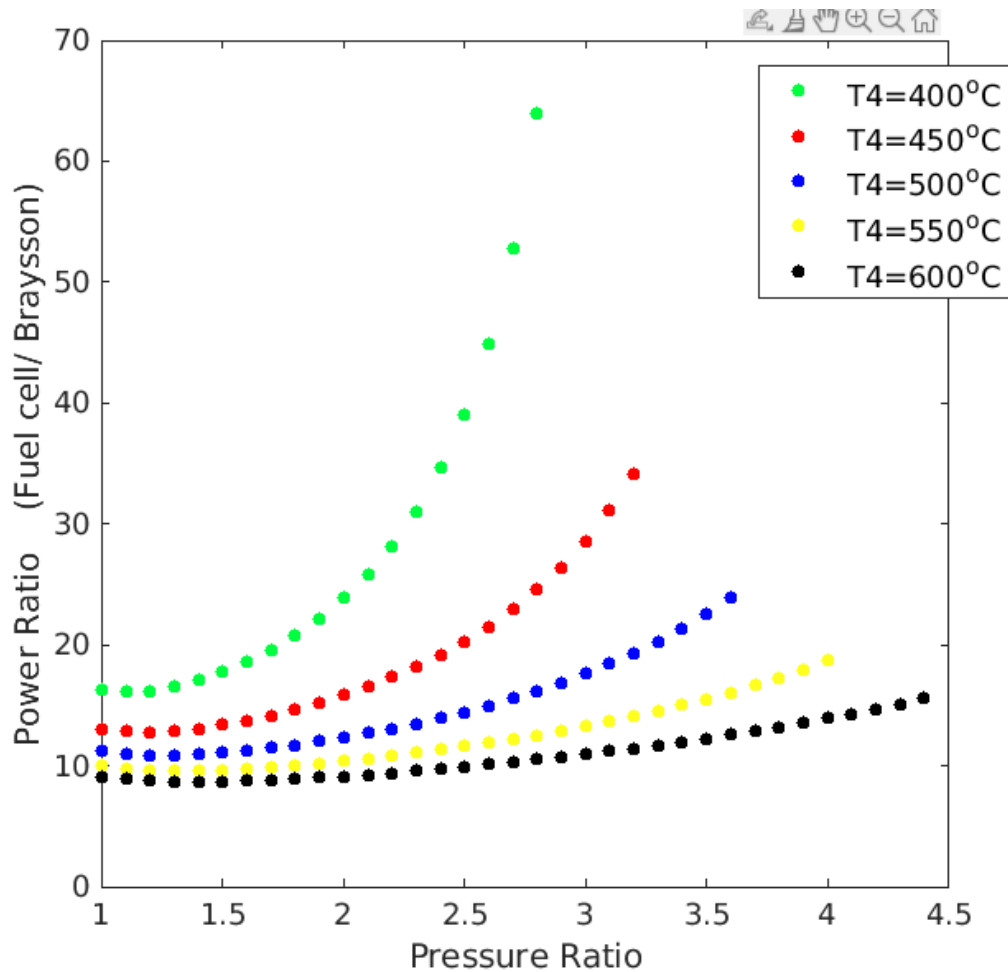


Fig 4.8 Power Ratio (Fuel cell/Braysson) vs. Pressure Ratio at different TIT

It can be observed from the figure 4.8 that power ratio (Fuel cell/Braysson cycle) first decreases till a particular pressure ratio and then increases.

Power outputs of both Braysson cycle and Fuel cell increase initially but the rate of increase in power output of Braysson cycle is more than that of the fuel cell with pressure ratio, these can be observed from the figures 4.6 & 4.7. So, the graph initially is decreasing. After a critical point, power output of Braysson cycle decreases and fuel cell increases with increase in pressure ratio. Therefore, the Power ratio (Fuel cell/Braysson cycle) graph keeps on increasing from then.

Power ratio (Fuel cell/Braysson cycle) decreases with increasing in TIT. This is because power outputs of both Braysson cycle and Fuel cell increase initially but the rate of increase in power output of Braysson cycle is more than that of the fuel cell with TIT.

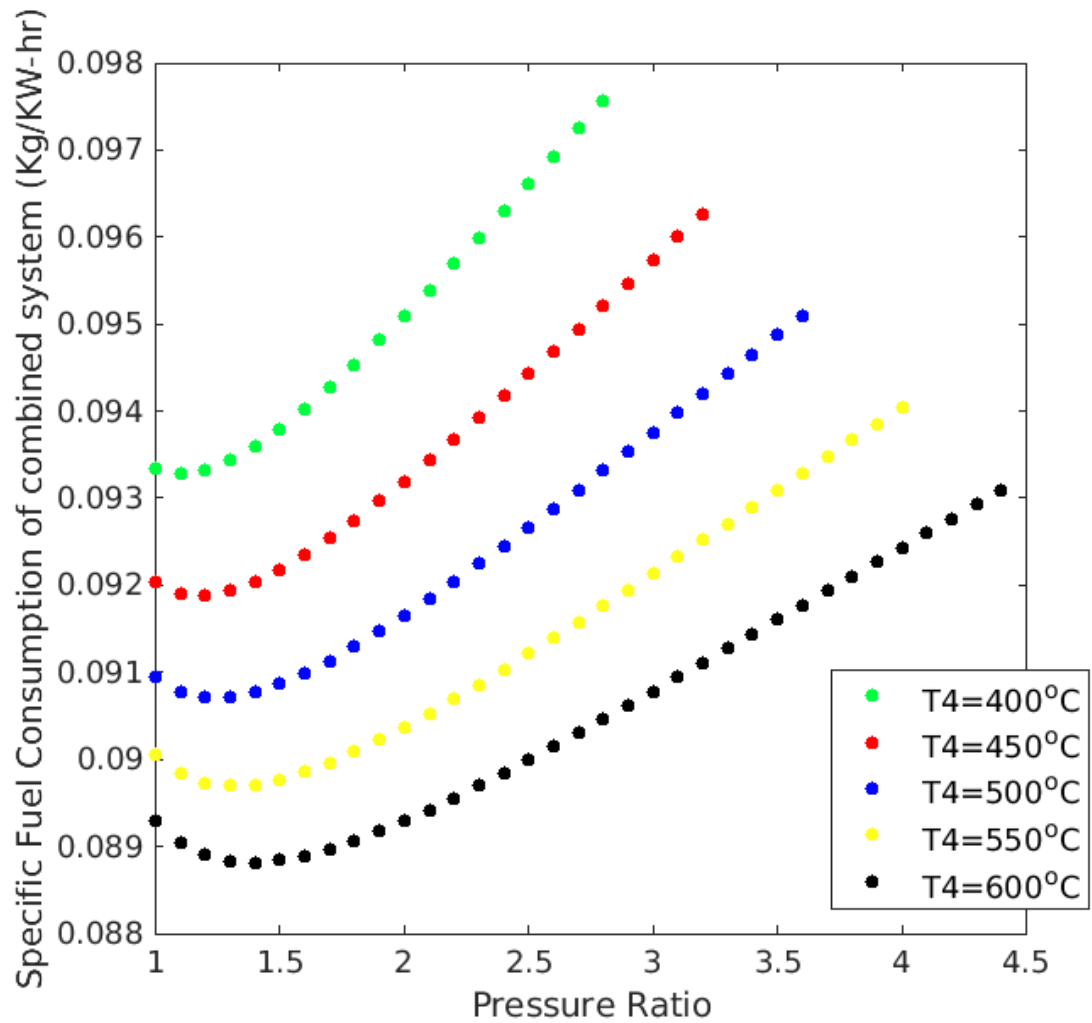


Fig 4.9 Specific Fuel Consumption of combined system (Kg/KW-hr) vs. Pressure Ratio at different TIT

It can be observed from the figure 4.9 that specific fuel consumption first decreases till a particular pressure ratio and then increases. It is because efficiencies first increase and then decrease with pressure ratio.

Specific fuel consumption decreases with increasing in T_4 . It is because efficiencies increase with increase in T_4 .

An optimum pressure ratio is found between 1 and 2 (nearly 1.4) where fuel consumption is least and efficiencies are maximum.

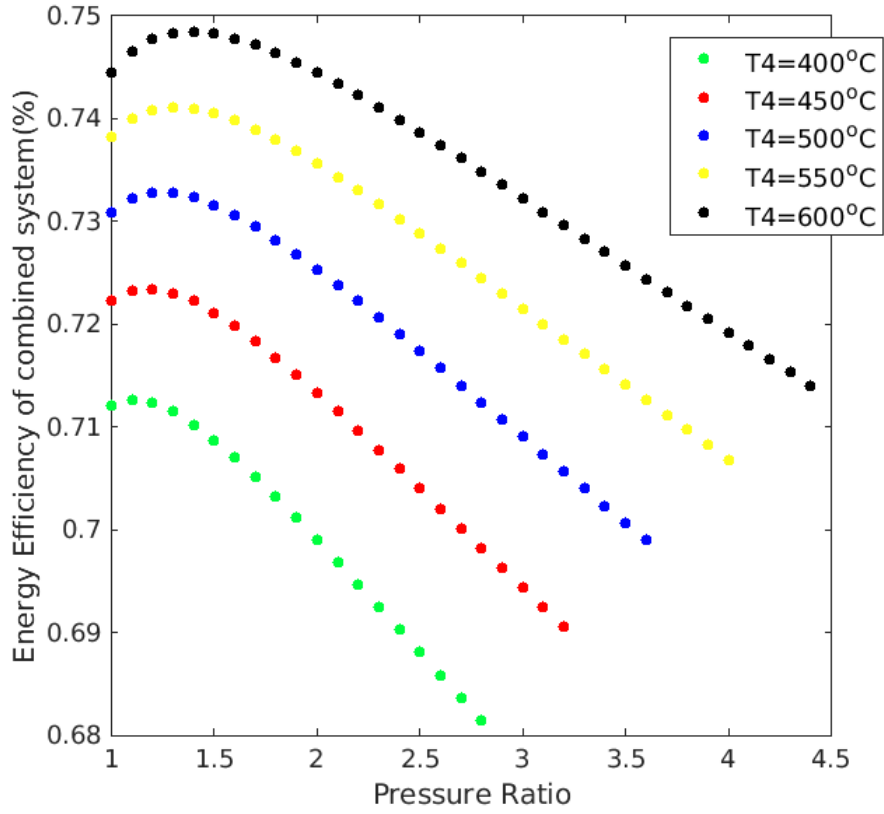


Fig 4.10 Energy Efficiency of combined system (%) vs. Pressure Ratio at different TIT

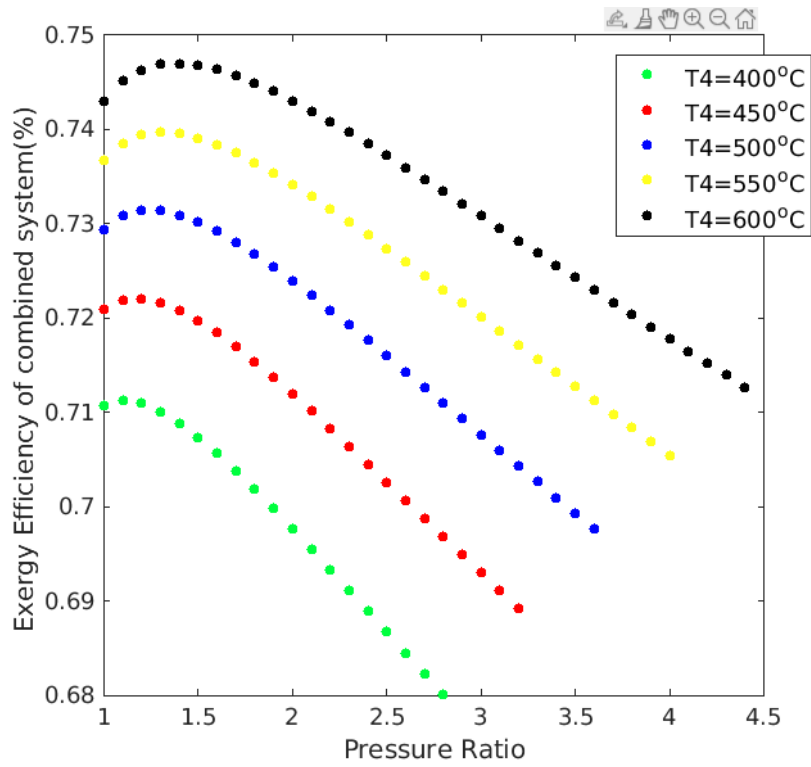


Fig 4.11 Exergy Efficiency of combined system (%) vs. Pressure Ratio at different TIT

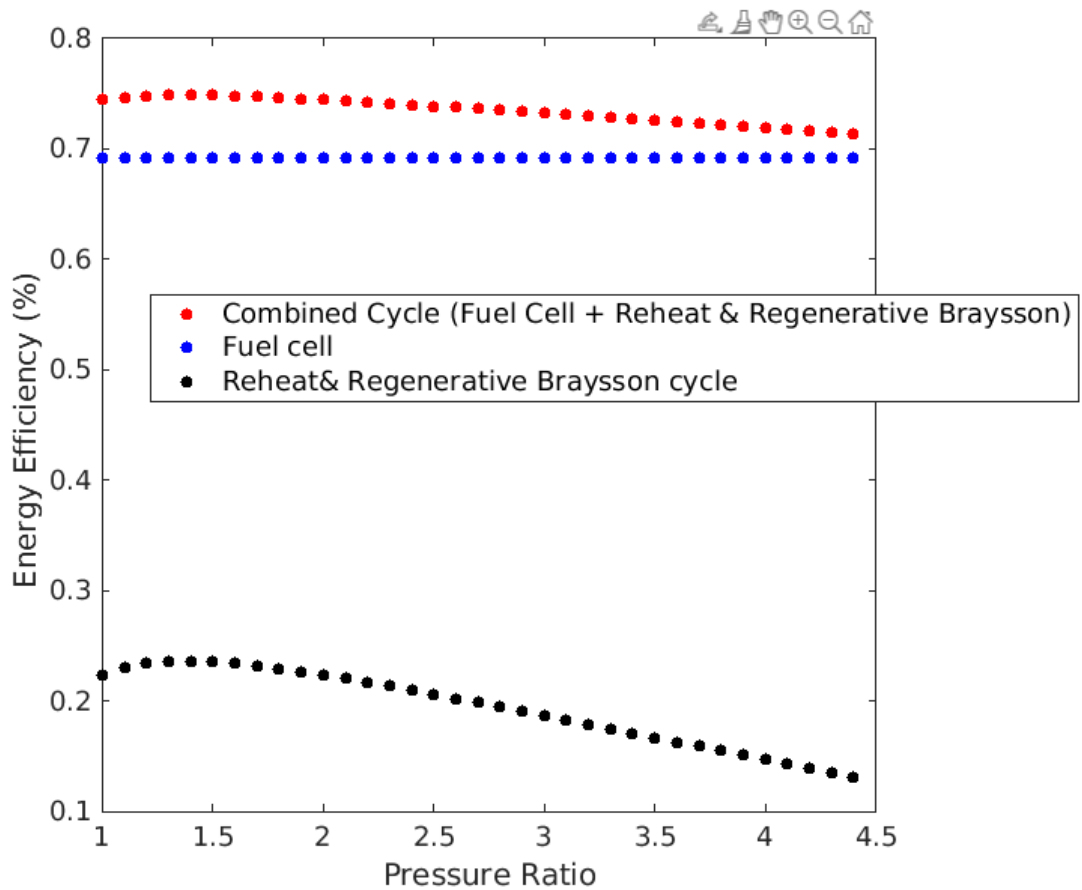


Fig 4.12 Energy Efficiency (%) vs Pressure Ratio

It can be observed from the figures 4.10, 4.11 & 4.12 that both the energy and exergy efficiencies of the combined cycle increase with increase in pressure ratio, then reach an optimum value and then decrease.

Both the energy and exergy efficiencies of the combined cycle increase with increase in T_4 value.

An optimum pressure ratio is found between 1 and 2 where maximum efficiency of the combined cycle is observed.

These plots are similar to those of the reheat and regenerative Braysson cycle because the energy and exergy efficiencies of the reheat and regenerative Braysson cycle depend upon pressure ratio and TIT as shown in figure 4.1 and 4.2 whereas these efficiencies of fuel cell as shown in figure 4.3 and 4.4 are independent of pressure ratio and TIT.

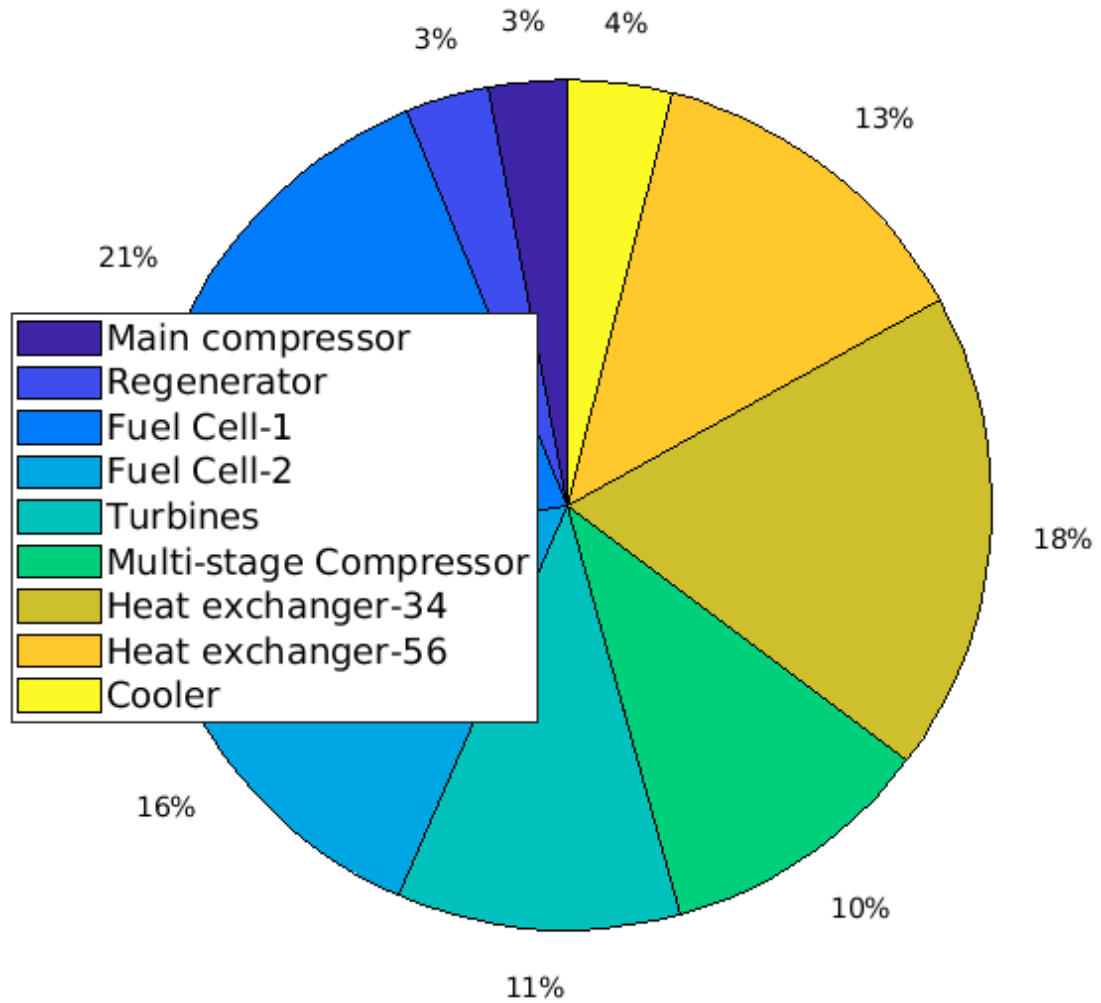


Fig 4.13 Pie chart representing component wise exergy destruction rates at an optimum pressure ratio of 1.4 and TIT=600°C

Component wise exergy destruction rates at the optimum pressure ratio of 1.4 and $T_4=600^\circ\text{C}$ value is shown in the figure 4.13.

It can be observed that most amount of exergy is destroyed in the cooler followed by the heat exchangers and then in turbines.

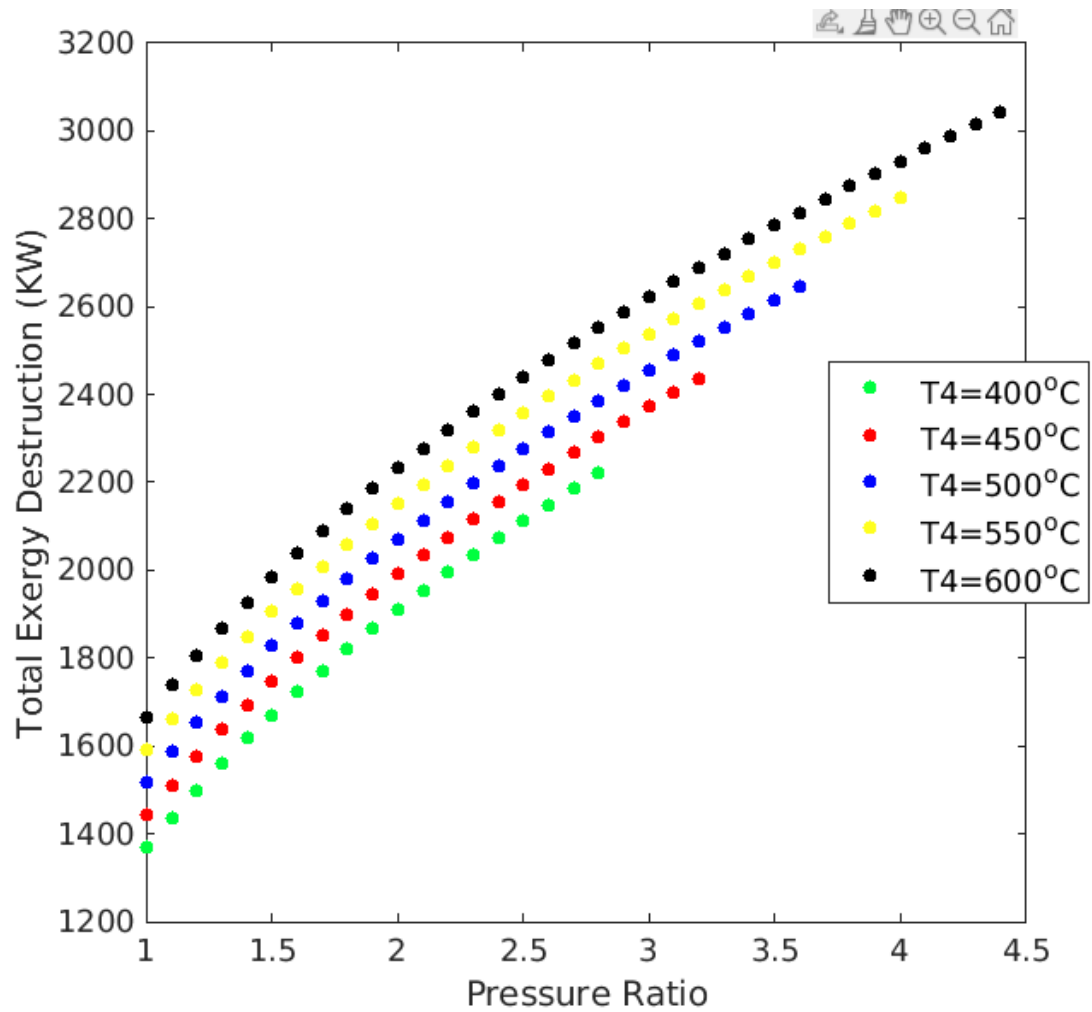


Fig 4.14 Total Exergy Destruction vs Pressure ratio at different TIT

It is found that as pressure ratio increases, total exergy destruction rate increases and as TIT increases, the total exergy destruction rate rate decreases.

Waste heat from fuel cell at 650 °C at TIT = 600 °C and $r_p=1.4$ from equation below is given by

$$((m_{H_2O} \cdot 0.8 \cdot q_{h1} \cdot (1 - (T_0/T))) + (m_{CO_2} \cdot 0.8 \cdot q_{h2} \cdot (1 - (T_0/T)))) = 4400 \text{ KW.}$$

The amount of work developed by reheat and regenerative Braysson cycle using this waste heat at TIT = 600 °C and $r_p=1.4$ is given by

$$(w_{o,p} \text{ of Braysson} - w_{i,p} \text{ of Braysson}) = 486 \text{ KW.}$$

The following observations are made from these charts:

Main Compressor: Exergy efficiency and exergy destruction of main compressor are independent of T_4 and hence remain constant.

Regenerator: Exergy efficiency is constant and exergy destruction rate increase with T_4 value. As T_4 increases, T_7 increases. So, irreversibility increases as the difference (T_7-T_2) increases and hence exergy destruction of the regenerator increases.

Fuel Cells: Maximum exergy efficiency is found in fuel cells among all the components.

Exergy efficiency is constant because it is independent of mass flow rate in the fuel cell from equations (13), (18), (19) and exergy destruction rate increase with T_4 value because as T_4 increases, mass flow rate in the fuel cell increases since (T_4-T_3) increases from equation (10) thereby increasing the exergy destruction rate.

Turbines: Exergy destruction rate is constant with T_4 value since at a given pressure ratio, T_4/T_5 is constant and also pressure ratio, P_4/P_7 remains constant. Exergy efficiency increases since exergy recovered increases as T_4 increases and exergy destroyed remains constant since it is independent of T_4 as T_5 is a function of T_4 and r_{p1} is a constant from equations (12), (26) and (27).

Multi stage Compressor: Exergy efficiency and exergy destruction of main compressor are independent of T_4 and hence remain constant.

Heat exchangers: Exergy efficiency increases and exergy destruction rate decreases with T_4 value. In Heat exchangers, as the temperature difference between the source and working fluid decreases, the exergy efficiency of the heat exchangers increases.

Cooler: Exergy efficiency of cooler is zero and exergy destruction of cooler increases with increase in T_4 value. In cooler, the exergy of cooling water is not recovered and is lost as waste heat to the environment. Hence it can be concluded that the exergy efficiency of the cooler is zero.

CHAPTER 5

5. CONCLUSIONS

Waste heat recovery from an ideal Molten Carbonate Fuel Cell (MCFC) using a Reheat and Regenerative Braysson cycle is analysed in this work. The following important conclusions are made:

- As maximum cycle temperature increases, corresponding value of limiting pressure ratio also increases.
- It can be observed that both the energy and exergy efficiencies of the combined cycle increase with increase in pressure ratio, then reach an optimum value and then decreases.
- Both the energy and exergy efficiencies of the combined cycle increases with increase in maximum cycle temperature value.
- In the analysis, molten carbonate fuel cell is assumed to operate at 650°C and the turbine inlet temperature (TIT) range of Braysson cycle is assumed as 400 to 600°C. It has been observed that there exist different optimum pressure ratio values for maximum power output and maximum efficiencies.
- Both the energy and exergy efficiencies of fuel cell are independent of pressure ratio.
- The power obtained from the fuel cell is 9 to 16 times higher than the power obtained from the waste heat through Braysson depending on the pressure ratio and TIT.
- Even when pressure ratio of main compressor is 1, this Brayssoncycle has an efficiency.
- The number of stages in the multistage compressor is fixed to 4.
- It is found that maximum efficiency occurs at back pressure of low pressure turbine at 0.2 bar for a pressure ratio value nearly 1.5.

- The combined system depicts energy efficiency in the range of 73% to 76% and that of the fuel cell is about 65%. Exergy destruction rates for the individual equipments and the total system are also obtained as a function of pressure ratio and TIT. The exergy destruction rates are found to be maximum in the heat transfer equipment and minimum in the fuel cell.
- The waste heat from the Molten Carbonate fuel cell is found to be 1354.6 KW at turbine inlet temperature of 600°C and at an optimum pressure ratio of 1.4. The power output of reheat and regenerative Braysson cycle obtained by recovering this waste heat is found to be 580 KW.

FUTURE SCOPE

A combined system of Molten Carbonate methane(fuel)-potassium carbonate (oxidiser) fuel cell & reheat and regenerative Braysson cycle in order to recover the waste heat is studied in this work with the fuel cell temperature constant at 650°C.

The same can be studied with different fuel cells like Phosphoric Acid Fuel cell (PAFC), Alkaline Fuel Cell (AFC), Solid Polymer Fuel Cell (SPFC), Solid Oxide Fuel Cell (SOFC), etc.

Also, the study can be conducted with the fuel cells operating at different temperatures.

CHAPTER 6

Environmental Impacts

At present, exponentially increasing demand of energy especially in fast growing economies, and the persistence in the use of fossil energy sources, impels to investigate new sustainable energy production and conversion systems. The interest in fuel cell (FC) technology is increasing in parallel with the increases of environmental concern about global warming, which calls for a worldwide reduction of carbon dioxide (CO₂) emissions. Fuel cells (FCs) are galvanic cells, in which the free energy of a chemical reaction is converted into electrical energy (via an electrical current). Because electrical energy is generated without combusting any fuel, FCs offer multiple environmental and technical benefits, making them a vital technology towards to a low emission energy supply. A wide range of FCs exist, typically classified by either their operating temperature or the type of electrolyte. High temperature FCs, such as Molten Carbonate Fuel Cells (MCFCs), are promoted as ultraclean and a favored solution suitable for stationary power generation, offering rich potential to reduce reliance on the already strained power grid, alleviating carbon footprint and providing a source of renewable energy.

MCFC environmental performance is heavily influenced by the current use of non-renewable energy and high material demand of rare minerals which generate high environmental burdens in the manufacturing stage, thereby confirming the prominent role of these processes in a comprehensive Life Cycle Analysis (LCA) study. The comparison of operational phases highlights that MCFCs are robust and able to compete with other mature technologies contributing substantially to airborne emissions reduction and promoting a switch to renewable fuels, however, further progress and market competitiveness urges adoption of an eco-efficiency philosophy to forge the link between environmental and economic concerns. Adopting a well-organized systematic research driven by life cycle models and eco-efficiency principles stakeholders will glean valuable information to make well balanced decisions for improving performance towards the concept 'producing more quality with less resources' and accelerate market penetration of the technology.

SUSTAINABLE DEVELOPMENT

Mother INDIA is abundant in renewable energy resources that can potentially fulfil its energy needs. However, the government is still trying to conquer its energy crisis by means of conventional energy technologies. An effective and sustainable long-term solution must be adopted in terms of renewable energy technologies. It is with regret that these resources have not been harvested, due to social, economic, and bureaucratic barriers. To strengthen the renewable energy technologies in, the public and private sectors should greatly devote investments in renewable energy technologies for creating a sustainable future. Fuel cell technology is one of the most promising renewable energy technologies due to its compatibilities with several renewable energy resources and being combustion-free. In addition, the diversity of FC technology makes it a suitable candidate to justify our future energy demands and sustainable development of the country. The fuel used in FC technology is highly effective compared to conventional fuels. In the future, we will expect that the cost of FCs will be largely reduced by the development of improved fuel storage techniques. Therefore, FC's hybrid systems will enact a brighter perspective of the country.

REFERENCES

- [1] Mehrpooya, M., Sayyad, S., & Zonouz, M. J. (2017). Energy, exergy and sensitivity analyses of a hybrid combined cooling, heating and power (CCHP) plant with molten carbonate fuel cell (MCFC) and Stirling engine. *Journal of Cleaner Production*, 148, 283–294. doi:10.1016/j.jclepro.2017.01.157
- [2] Frost TH, Anderson A, Agnew B. A hybrid gas turbine cycle (Brayton/Ericsson): an alternative to conventional combined gas and steam turbine power plant. *Proc Institute of Mechanical Engineering Part A J Power Energy* 1997;211(2):121e31.
- [3] R. Chandramouli, M.S.S. Srinivasa Rao, K. Ramji. Energy and exergy based thermodynamic analysis of reheat and regenerative Braysson cycle.
- [4] Zheng J, Sun F, Chen L, Wu C. Exergy analysis for a Braysson cycle. *Exergy IntJ*2001;1(1):41e5.
- [5] Zheng J, Chen L, Sun F, Wu C. Powers and efficiency performance of an Endo reversible Braysson cycle. *Int J Therm Sci* 2002;41:201e5.
- [6] Sreenivas B, Chandramouli R, Sudhakar I, Thulasiram AR. Second law analysis irreversible Braysson cycle. *Int J Exergy* 2009;6(6):826e36.
- [7] Duan, L., Yue, L., Feng, T., Lu, H., & Bian, J. (2016). Study on a novel pressurized MCFC hybrid system with CO₂ capture. *Energy*, 109, 737–750. doi:10.1016/j.energy.2016.05.074
- [8] Salehi, A., Mousavi, S. M., Fasihfar, A., & Ravanbakhsh, M. (2019). Energy, exergy, and environmental (3E) assessments of an integrated molten carbonate fuel cell (MCFC), Stirling engine and organic Rankine cycle (ORC) cogeneration system fed by a biomass-fueled gasifier. doi:10.1016/j.ijggc.2011.10.001.
- [9] Jarchlouei M.A., Chitsaz A., Mahmoudi S.M.S., Rosen M.A., & Bafekr, S.H. (2021). Gibbs energy minimization using Lagrange method of undetermined multipliers for electrochemical and thermodynamic modeling of a MCFC with internal steam reforming. *Energy Conversion and Management*, 228, 113594. doi:10.1016/j.enconman.2020.113594
- [10] Ust Yasin, Yilmaz T. Performance analysis of an Endo reversible Braysson cycle based on the ecological criterion. *Turk J Eng Env Sci* 2005;29:271e8.

- [11] Campanari, S., Chiesa, P., Manzolini, G., Giannotti, A., Federici, F. (2011). Application of MCFCs for active CO₂ capture within natural gas combined cycles. *Energy Procedia*. doi:10.1016/j.egypro.2011.01.179
- [12] Campanari, Bedont, P., & Parodi, F. (2011). Application of MCFCs for active CO₂ capture within natural gas combined cycles. *Energy Procedia*, 4,1235–1242
- [13] Junlin Zheng, Fengrui Sun, Lingen Chen, Chih Wu., Exergy analysis for a Braysson cycle.
- [14] Desideri, U., Proietti, S., Cinti, G., Sdringola, P., & Rossi, C. (2011). Analysis of pollutant emissions from cogeneration and district heating systems aimed to a feasibility study of MCFC technology for carbon dioxide separation as retrofitting of existing plants. *International Journal of Greenhouse Gas Control*, 5(6),1663–1673. doi:10.1016/j.ijggc.2011.10.001.
- [15] Haghghat Mamaghani, A., Najafi, B., Shirazi, A., & Rinaldi, F. (2015). 4E analysis and multi-objective optimization of an integrated MCFC (molten carbonate fuel cell) and ORC (organic Rankine cycle) system. *Energy*, 82, 650–663. doi:10.1016/j.energy.2015.01.074
- [16] Mehrpooya, M., Khodayari, R., Ali Moosavian, S. M., & Dadak, A. (2020). Optimal design of molten carbonate fuel cell combined cycle power plant and thermophotovoltaic system. *Energy Conversion and Management*, 221, 113177. doi:10.1016/j.enconman.2020.113177
- [17] Selman J. R. (2006), 'Molten-salt fuel cells-Technical and economic challenges', *Journal of Power Sources*, (160), pp. 852-867.
- [18] Tomczyk P. (2006), 'MCFC versus other fuel cells—Characteristics, technologies and prospects', *Journal of Power Sources*, 160, pp. 858-862.
- [19] Zhang Shiyan, Chan Jincon, Lin Guoxing. (2005). Performance characteristics of irreversible solar driven Braysson heat engine at maximum efficiency.
- [20] Georgiou Demos P, Xenos Triantafyllos. The process of isothermal compression of gasses at sub-atmospheric pressures through regulated water injection in Braysson cycles. *Applied Thermal Engineering* 2011;31(14e15):2205e12.
- [21] Chandramouli R, Srinivasa Rao MSS, Ramji K. Energy and exergy based thermodynamic analysis of reheat and regenerative Braysson cycle. *Energy* 2015. <http://dx.doi.org/10.1016/j.energy.2015.07.017>

APPENDIX

MATLAB CODE

Main programming

```

T=650+273.15;
T1=298.15;
%t4=700;
j=1;
for t4=400:50:600
%t4=750;
T4=t4+273.15;
p7=0.4;
pat=1.013;
eta1c=0.8;
N=2;
deltaG1=11005.055; % value of h2o at 650 degreecelcius (KJ/kg);
deltaH1=13814.63;% value of h2o at 650 degree celcius (KJ/kg);

deltaG2=3602.081; % value of co2 at 650 degreecelcius (KJ/kg);
deltaH2=8390.727;% value of co2 at 650 degree celcius (KJ/kg);
deltaG=deltaG1+deltaG2;
deltaH=deltaH1+deltaH2;

cesCH4=51810.7;%chemical exergy of CH4 (KJ/kg);
ceso=612.82;%chemical exergy of K2CO3 (KJ/kg);
Cph=5.19;%CP of helium in KJ/kgK;
mf=1;%mf is mass flow rate of braysson = 1kg/s;
qh1=(deltaH1-deltaG1); % qh is heat from fuel cell;
qh2=(deltaH2-deltaG2); % qh is heat from fuel cell;

etareg=0.8;
etat=0.8;
etac=0.8;
%rp=4;
gama=1.667;
T6=T4;
T9=T1;
T0=T1;
%for N=1:1:100
i=1;
for rp=1:1:100
    p4=rp*pat;
    rp1=sqrt(p4/p7);
    rpo=pat/p7;

```

```

T2=T1+T1*(rp^((gama-1)/gama)-1)/etac;

T5=T4+etac*T4*(rp1^((1-gama)/(gama))-1);
if T2<T5
pr(i,1)=rp;
T7=T5;
T3=etareg*(T7-T2)+T2;
T8=T7-T3+T2;
%if T3<T8
Ta=T9+(T9*((rpo^((gama-1)/(N*gama)))-1)/eta1c);
QH1= mf*Cph*(T4-T3)/0.8;
mco21=QH1/(qh2+(9/11)*qh1);
mh2o1=(9/11)*mco21;

mf1=(16/44)*mco21;
QH2= mf*Cph*(T6-T5)/0.8;
mco22=QH2/(qh2+(9/11)*qh1);
mh2o2=(9/11)*mco22;

mf2=(16/44)*mco22;
mfCH41=mf1;
mfCH42=mf2;
mfo1=4*mfCH41;
mfo2=4*mfCH42;

esc=Cph*(T2-T1);%Exergy supplied for compressor;
erc=Cph*(T2-T1)-T0*Cph*(log(T2/T1)-((gama-1)*log(rp)/gama));%Exergy
recovered;
edc=esc-erc;%Exergy destroyed;
eeffc=erc/esc;%Exergy efficiency of compressor;

%Exergy efficiency of regenerator;
eeffr=((T3-T2)-T0*log(T3/T2))/((T7-T8)-T0*log(T7/T8));
edr=Cph*((T7-T8)-T0*log(T7/T8))-Cph*((T3-T2)-T0*log(T3/T2));

%Exergy efficiency of fuel cell;

eeffc1=(((mh2o1*((qh1)*(1-(T0/T))+deltaG1)))+(mco21*(qh2*(1-
(T0/T))+deltaG2)))/((mfCH41*cesCH4)+(mfo1*ceso));
eeffc2=(((mh2o2*((qh1)*(1-(T0/T))+deltaG1)))+(mco22*(qh2*(1-
(T0/T))+deltaG2)))/((mfCH42*cesCH4)+(mfo2*ceso));

eeffwoqhfc1=(((mh2o1*deltaG1)+(mco21*deltaG2))/((mfCH41*cesCH4)+(mfo1*ces
o));
eeffwoqhfc2=(((mh2o2*deltaG1)+(mco22*deltaG2))/((mfCH42*cesCH4)+(mfo2*ces
o));

edfc1=(((mfCH41*cesCH4)+(mfo1*ceso))-(((mh2o1*((qh1)*(1-
(T0/T))+deltaG1)))+(mco21*((qh2)*(1-(T0/T))+deltaG2))));

```

```
edfc2=((mfCH42*cesCH4)+(mfo2*ceso))-(((mh2o2*((qh1)*(1-
(T0/T))+deltaG1)))+(mco22*((qh2)*(1-(T0/T))+deltaG2))));
```

```
edfwoqhc1=((mfCH41*cesCH4)+(mfo1*ceso)-
((mh2o1*deltaG1)+(mco21+deltaG2));
```

```
edfwoqhc2=((mfCH42*cesCH4)+(mfo2*ceso)-
((mh2o2*deltaG1)+(mco22+deltaG2));
```

```
edwh1=((mh2o1*0.2*qh1*(1-(T0/T)))+(mco21*0.2*qh2*(1-(T0/T)));%exergy
destruction by gases(waste heat) in fuel cell 1
```

```
edwh2=((mh2o2*0.2*qh1*(1-(T0/T)))+(mco22*0.2*qh2*(1-(T0/T)));%exergy
destruction by gases(waste heat) in fuel cell 2
```

```
%Exergy efficiency of Turbine;
```

```
est=2*(Cph*(T4-T5)-Cph*T0*(log(T4/T5)-((gama-1)*log(rp1)/gama)));
```

```
ert=2*(Cph*(T4-T5));
```

```
edt=est-ert;
```

```
eefft=ert/est;
```

```
%Exergy efficiency of multistage compressor with intercooling;
```

```
first=N*Cph*T9*(rpo^((gama-1)/(gama*N))-1)/eta1c;
```

```
sec=-N*Cph*T0*(log(1+((rpo^((gama-1)/(gama*N))-1)/eta1c)));
```

```
thir=(N*Cph*T0*(gama-1)*log(rpo))/(gama*N);
```

```
ermc=first+sec+thir;
```

```
%ermc=N*Cph*((T9*(rpo^((gama-1)/(gama*N))-1)/eta1c)-T0*log(1+((rpo^((gama-
1)/(gama*N))-1)/eta1c)+T0*((gama-1)*log(rpo)/(gama*N)));
```

```
ermi=(N-1)*Cph*((Ta-T9)-T0*log(1+((rpo^((gama-1)/(gama*N))-1)/eta1c)));
```

```
ermct=ermc-ermi;
```

```
esmct=N*Cph*(Ta-T9);
```

```
edmct=esmct-ermct;
```

```
eeffmct=ermct/esmct;
```

```
%exergy in heating of the fluid (3-4)& (5-6) process
```

```
erhf34=Cph*((T4-T3)-T0*(log(T4/T3)));
```

```
eshf34=(mh2o1*(qh1)*(1-(T0/T))+mco21*(qh2)*(1-(T0/T)));
```

```
edhf34=eshf34-erhf34;
```

```
eehf34=erhf34/eshf34;
```

```
erhf56=Cph*((T6-T5)-T0*(log(T6/T5)));
```

```
eshf56=(mh2o2*(qh1)*(1-(T0/T))+mco22*(qh2)*(1-(T0/T)));
```

```
edhf56=eshf56-erhf56;
```

```
eehf56=erhf56/eshf56;
```

```
edcool=Cph*((T8-T9)-T0*log(T8/T9));
```

```
Wopb=Cph*(T4-T5)+Cph*(T6-T7);
```

```
Winb=Cph*(T2-T1)+N*Cph*(Ta-T9);
```

```
Wopf=((mh2o1+mh2o2)*deltaG1+(mco21+mco22)*deltaG2);
```

```
Qin=deltaH1*(mh2o1+mh2o2)+deltaH2*(mco21+mco22);
```

```
%Effb=Wopb/qh;
```

```
%p=Wopb-Winb;
```

```
Efff=deltaG/deltaH;
```

```
%Effb=(Wopb-Winb)/Qin;
```

```
%Effov=(Wopb+Wopf-Winb)/Qin;
```

```
Effb=(Wopb-Winb)/(qh1*(mh2o1+mh2o2)+qh2*(mco21+mco22));
```

```

Effov=(Wopb+Wopf-Winb)/Qin;
% Total Exergy efficiency of Braysson and Fuel cell cycle;
tes=((mfCH41*cesCH4)+(mfo1*ceso))+((mfCH42*cesCH4)+(mfo2*ceso));%total
exergy supplied;
NW=Wopb+Wopf-Winb;
NWB=Wopb-Winb;
TFC=(mfCH41+mfCH42)*3600;
SFC=TFC/NW;
Workratio=Wopf/NWB;
eeffov=(Wopb+Wopf-
Winb)/(((mfCH41*cesCH4)+(mfo1*ceso))+((mfCH42*cesCH4)+(mfo2*ceso)));
Texd=(1-eeffov)*tes;% Total Exergy Destroyed;
ECOP=NW/Texd;

ted=edc+edr+edfc1+edfc2+edt+edmct+edhf34+edhf56+edcool;%sum of exergy
destruction of individual;

difference=Texd-ted;
percentage=difference*100/tes;
%plot(rp,Effov,'b.',rp,Efff,'r.',rp,Effb,'g.')
%plot(rp,eeffov,'m.')
%plot(rp,eeffov,'r.',rp,Effov,'b.')

%hold on
tesb=eshf34+eshf56;
erb=NWB;
eeffb=erb/tesb;
percentage1(i,1)=percentage;
ECOP1(i,1)=ECOP;
ted1(i,1)=Texd;
ted2(j,i)=Texd;
eeffb1(i,1)=eeffb;
eeffc11(i,1)=eeffc1;
eeffc21(i,1)=eeffc2;

Effov1(i,1)=Effov;
eeffov1(i,1)=eeffov;
Efff1(i,1)=Efff;
Effb1(i,1)=Effb;
WR(i,1)=Workratio;
SFC1(i,1)=SFC;
Wopf1(i,1)=Wopf;
NWB1(i,1)=NWB;
NW1(i,1)=NW;
i=i+1;
else
%end
%else
end
if t4==400

```

```

    if rp==1.4

figure(6)
    fig = figure(6);
    u = fig.Color;
    fig.Color = 'w';
    pie([edc edr edfc1 edfc2 edt edmct edhf34 edhf56 edcool])
    legend({'Main compressor','Regenerator','Fuel Cell-1','Fuel Cell-2','Turbines','Multi-
stage Compressor','Heat exchanger-34','Heat exchanger-
56','Cooler'},'location','best','fontsize',13)
    end
end
hold on
end
edc1(j,1)=edc;
edr1(j,1)=edr;
edfc11(j,1)=edfc1;
edfc21(j,1)=edfc2;
edt1(j,1)=edt;
edmct1(j,1)=edmct;
edhf341(j,1)=edhf34;
edhf561(j,1)=edhf56;
edcool1(j,1)=edcool;
eeffc1(j,1)=eeffc;
eeffr1(j,1)=eeffr;
eeffc11(j,1)=eeffc1;
eeffc21(j,1)=eeffc2;
eefft1(j,1)=eefft;
eeffmct1(j,1)=eeffmct;
eehf341(j,1)=eehf34;
eehf561(j,1)=eehf56;
eecool(j,1)=0;
j=j+1;

figure(1)
fig = figure(1);
u = fig.Color;
fig.Color = 'w';

%p=plot(pr,Effov1,'k.',pr,Eff1,'r.','markersize',8);
if t4==400
    plot(pr,Effov1,'g.','markersize',20);
%p(1).Marker = '*';
%p(2).Marker = '*';
end
if t4==450
    plot(pr,Effov1,'r.','markersize',20);
%p(1).Marker = 'o';
%p(2).Marker = 'o';

```

```

end
if t4==500
    plot(pr,Effov1,'b.','markersize',20);
%p(1).Marker = '.';
%p(2).Marker = '.';
end
if t4==550
    plot(pr,Effov1,'y.','markersize',20);
%p(1).Marker = 'p';
%p(2).Marker = 'p';
end
if t4==600
    plot(pr,Effov1,'k.','markersize',20);
%p(1).Marker = 'p';
%p(2).Marker = 'p';
end
legend({' T4=400^{o}C',' T4=450^{o}C',' T4=500^{o}C',' T4=550^{o}C','
T4=600^{o}C'},'location','best','fontsize',13)

%legend({'Hybrid Cycle (Fuel Cell + Reheat & Regenerative Braysson)','Fuel
Cell'},'location','best','fontsize',13)
xlabel('Pressure Ratio','fontsize',13)
ylabel('Energy Efficiency of combined system(%)','fontsize',13)
%axis([1 5 0.73 0.83])
axis square
ax = gca;
c = ax.FontSize;
ax.FontSize = 13;
hold on
figure(2)
fig = figure(2);
u = fig.Color;
fig.Color = 'w';
%p2=plot(pr,Effov1,'g.','pr,effov1','r.','markersize',8)
if t4==400
    plot(pr,effov1,'g.','markersize',20)
%p2(1).Marker = '*';
%p2(2).Marker = '*';
end
if t4==450
    plot(pr,effov1,'r.','markersize',20)
%p2(1).Marker = 'o';
%p2(2).Marker = 'o';
end
if t4==500
    plot(pr,effov1,'b.','markersize',20)
%p2(1).Marker = '.';
%p2(2).Marker = '.';
end

```



```

if t4==550
    plot(pr,eeffov1,'y.','markersize',20)
%p2(1).Marker = 'p';
%p2(2).Marker = 'p';
end
if t4==600
    plot(pr,eeffov1,'k.','markersize',20)
%p2(1).Marker = 'p';
%p2(2).Marker = 'p';
end
legend({' T4=400^{o}C',' T4=450^{o}C',' T4=500^{o}C',' T4=550^{o}C','
T4=600^{o}C'},'location','best','fontsize',13)
%legend({'Energy efficiency of Hybrid cycle','Exergy efficiency of Hybrid
cycle'},'location','best','fontsize',13)
xlabel('Pressure Ratio','fontsize',13)
ylabel('Exergy Efficiency of combined system(%) ','fontsize',13)
%axis([1 5 0.8 0.88])
axis square
ax = gca;
c = ax.FontSize;
ax.FontSize = 13;
hold on
if t4==950
figure(3)
fig = figure(3);
u = fig.Color;
fig.Color = 'w';
plot(pr,Effov1,'r.',pr,Eff1,'b.',pr,Effb1,'k.','markersize',20)
legend({'Combined Cycle (Fuel Cell + Reheat & Regenerative Braysson)','Fuel
cell','Reheat& Regenerative Braysson cycle'},'location','best','fontsize',13)
xlabel('Pressure Ratio','fontsize',13)
ylabel('Energy Efficiency (%) ','fontsize',13)
%axis([1 5 0.1 0.88])
axis square
ax = gca;
c = ax.FontSize;
ax.FontSize = 13;
hold on
end
figure(4)
fig = figure(4);
u = fig.Color;
fig.Color = 'w';
%p4=plot(pr,WR,'k.','markersize',8)
if t4==400
    plot(pr,WR,'g.','markersize',20)
%p4(1).Marker = '*';

end
if t4==450

```

```

    plot(pr,WR,'r.','markersize',20)
%p4(1).Marker = 'o';
End
if t4==500
    plot(pr,WR,'b.','markersize',20)
%p4(1).Marker = '.';
end
if t4==550
    plot(pr,WR,'y.','markersize',20)
%p4(1).Marker = 'p';
end
if t4==600
    plot(pr,WR,'k.','markersize',20)
%p4(1).Marker = 'p';
end
%legend({'Powerratio of Fuel cell Vs Reheat & Regenerative Braysson
cycle'},'location','best','fontsize',13)
xlabel('Pressure Ratio','fontsize',13)
ylabel('Power Ratio (Fuel cell/ Braysson)','fontsize',13)
legend({' T4=400^{o}C',' T4=450^{o}C',' T4=500^{o}C',' T4=550^{o}C','
T4=600^{o}C'},'location','best','fontsize',13)
%axis([1 5 0.1 0.88])
axis square
ax = gca;
c = ax.FontSize;
ax.FontSize = 13;
hold on
figure(5)
fig = figure(5);
u = fig.Color;
fig.Color = 'w';
%p5=plot(pr,SFC1,'k.','markersize',8)
if t4==400
    plot(pr,SFC1,'g.','markersize',20)
%p5(1).Marker = '*';
end
if t4==450
    plot(pr,SFC1,'r.','markersize',20)
%p5(1).Marker = 'o';
end
if t4==500
    plot(pr,SFC1,'b.','markersize',20)
%p5(1).Marker = '.';
end
if t4==550
    plot(pr,SFC1,'y.','markersize',20)
%p5(1).Marker = 'p';
end
if t4==600
    plot(pr,SFC1,'k.','markersize',20)

```

```

%p5(1).Marker = 'p';
end
%legend({'Powerratio of Fuel cell Vs Reheat & Regenerative Braysson
cycle'},'location','best','fontsize',13)
xlabel('Pressure Ratio','fontsize',13)
ylabel('Specific Fuel Consumption of combined system (Kg/KW-hr)','fontsize',13)
legend({' T4=400^{o}C',' T4=450^{o}C',' T4=500^{o}C',' T4=550^{o}C','
T4=600^{o}C'},'location','best','fontsize',13)
%axis([1 5 0.1 0.88])
axis square
ax = gca;
c = ax.FontSize;
ax.FontSize = 13;
hold on
%pause
figure(7)
fig = figure(7);
u = fig.Color;
fig.Color = 'w';
%p7=plot(pr,Wopf1,'g.',pr,NWB1,'r.','markersize',8)
if t4==400
    plot(pr,Wopf1,'g.','markersize',20)
%p7(1).Marker = '*';
%p7(2).Marker = '*';
end
if t4==450
    plot(pr,Wopf1,'r.','markersize',20)
%p7(1).Marker = 'o';
%p7(2).Marker = 'o';
end
if t4==500
    plot(pr,Wopf1,'b.','markersize',20)
%p7(1).Marker = '.';
%p7(2).Marker = '.';
end
if t4==550
    plot(pr,Wopf1,'y.','markersize',20)
%p7(1).Marker = 'p';
%p7(2).Marker = 'p';
end
if t4==600
    plot(pr,Wopf1,'k.','markersize',20)
%p7(1).Marker = 'p';
%p7(2).Marker = 'p';
end
%legend({'Energy efficiency of Hybrid cycle','Exergy efficiency of Hybrid
cycle'},'location','best','fontsize',13)
xlabel('Pressure Ratio','fontsize',13)
ylabel('Power Output of Fuel cell(KW) ','fontsize',13)

```

```

legend({' T4=400^{o}C',' T4=450^{o}C',' T4=500^{o}C',' T4=550^{o}C','
T4=600^{o}C'},'location','best','fontsize',13)
%axis([1 6 6000 15000])
%axis square
ax = gca;
c = ax.FontSize;
ax.FontSize = 13;
hold on
figure(8)
%plot(pr,NWB1,'r.','markersize',8)
fig = figure(8);
u = fig.Color;
fig.Color = 'w';
%p9=plot(pr,Efff1,'k.','markersize',8)
if t4==400
%p9(1).Marker = '*';
plot(pr,NWB1,'g.','markersize',20)
end
if t4==450
%p9(1).Marker = 'o';
plot(pr,NWB1,'r.','markersize',20)
end
if t4==500
%p9(1).Marker = '.';
plot(pr,NWB1,'b.','markersize',20)
end
if t4==550
%p9(1).Marker = 'p';
plot(pr,NWB1,'y.','markersize',20)
end
if t4==600
%p9(1).Marker = 'p';
plot(pr,NWB1,'k.','markersize',20)
end
%legend({'Powerratio of Fuel cell Vs Reheat & Regenerative Braysson
cycle'},'location','best','fontsize',13)
xlabel('Pressure Ratio','fontsize',13)
ylabel('Power Output of Reheat & Regenerative Braysson(KW)','fontsize',13)
legend({' T4=400^{o}C',' T4=450^{o}C',' T4=500^{o}C',' T4=550^{o}C','
T4=600^{o}C'},'location','best','fontsize',13)
%axis([1 5 0.1 0.88])
axis square
%axis([1 6 .7 .8])
ax = gca;
c = ax.FontSize;
ax.FontSize = 13;
hold on
figure(9)
fig = figure(9);
u = fig.Color;

```

```

fig.Color = 'w';
%p9=plot(pr,Efff1,'k.','markersize',8)
if t4==400
%p9(1).Marker = '*';
plot(pr,Efff1,'gp','markersize',15)
end
if t4==450
%p9(1).Marker = 'o';
plot(pr,Efff1,'r*','markersize',15)
end
if t4==500
%p9(1).Marker = '.';
plot(pr,Efff1,'bo','markersize',15)
end
if t4==550
%p9(1).Marker = 'p';
plot(pr,Efff1,'y^','markersize',15)
end
if t4==600
%p9(1).Marker = 'p';
plot(pr,Efff1,'k.','markersize',15)
end
%legend({'Powerratio of Fuel cell Vs Reheat & Regenerative Braysson
cycle'},'location','best','fontsize',13)
xlabel('Pressure Ratio','fontsize',13)
ylabel('Energy efficiency of Fuel Cell','fontsize',13)
legend({' T4=400^{o}C',' T4=450^{o}C',' T4=500^{o}C',' T4=550^{o}C','
T4=600^{o}C'},'location','best','fontsize',13)
%axis([1 5 0.1 0.88])
%axis square
%axis([1 6 .7 .8])
ax = gca;
c = ax.FontSize;
ax.FontSize = 13;
hold on
figure(10)
fig = figure(10);
u = fig.Color;
fig.Color = 'w';
%p10=plot(pr,eeffc11,'k.','markersize',8)
if t4==400
%p10(1).Marker = '*';
plot(pr,eeffc11,'gp','markersize',15)
end
if t4==450
%p10(1).Marker = 'o';
plot(pr,eeffc11,'ro','markersize',15)
end
if t4==500
%p10(1).Marker = '.';

```

```

plot(pr,eeffc11,'b*','markersize',15)
end
if t4==550
%p10(1).Marker = 'p';
plot(pr,eeffc11,'y^','markersize',15)
end
if t4==600
%p10(1).Marker = 'p';
plot(pr,eeffc11,'k.','markersize',15)
end
%legend({'Powerratio of Fuel cell Vs Reheat & Regenerative Braysson
cycle'},'location','best','fontsize',13)
xlabel('Pressure Ratio','fontsize',13)
ylabel('Exergy efficiency of Fuel Cell','fontsize',13)
legend({' T4=400^{o}C',' T4=450^{o}C',' T4=500^{o}C',' T4=550^{o}C','
T4=600^{o}C'},'location','best','fontsize',13)
%axis([1 5 0.1 0.88])
%axis square
%axis([1 6 .9 1])
ax = gca;
c = ax.FontSize;
ax.FontSize = 13;
hold on
figure(11)
fig = figure(11);
u = fig.Color;
fig.Color = 'w';
%p10=plot(pr,eeffc11,'k.','markersize',8)
if t4==400
%p10(1).Marker = '*';
plot(pr,Effb1,'g.','markersize',20)
end
if t4==450
%p10(1).Marker = 'o';
plot(pr,Effb1,'r.','markersize',20)
end

if t4==500
%p10(1).Marker = '.';
plot(pr,Effb1,'b.','markersize',20)
end
if t4==550
%p10(1).Marker = 'p';
plot(pr,Effb1,'y.','markersize',20)
end
if t4==600
%p10(1).Marker = 'p';
plot(pr,Effb1,'k.','markersize',20)
end

```

```

%legend({'Powerratio of Fuel cell Vs Reheat & Regenerative Braysson
cycle'},'location','best','fontsize',13)
xlabel('Pressure Ratio','fontsize',13)
ylabel('Energy efficiency of Reheat and Regenerative Braysson cycle','fontsize',13)
legend({' T4=400^{o}C',' T4=450^{o}C',' T4=500^{o}C',' T4=550^{o}C','
T4=600^{o}C'},'location','best','fontsize',13)
%axis([1 5 0.1 0.88])
axis square
%axis([1 6 .9 1])
ax = gca;
c = ax.FontSize;
ax.FontSize = 13;
hold on
figure(12)
fig = figure(12);
u = fig.Color;
fig.Color = 'w';
%p10=plot(pr,eeffc11,'k.','markersize',8)
if t4==400
%p10(1).Marker = '*';
plot(pr,eeffb1,'g.','markersize',20)
end
if t4==450
%p10(1).Marker = 'o';
plot(pr,eeffb1,'r.','markersize',20)
end
if t4==500
%p10(1).Marker = '.';
plot(pr,eeffb1,'b.','markersize',20)
end
if t4==550
%p10(1).Marker = 'p';
plot(pr,eeffb1,'y.','markersize',20)
end
if t4==600
%p10(1).Marker = 'p';
plot(pr,eeffb1,'k.','markersize',20)
end
%legend({'Powerratio of Fuel cell Vs Reheat & Regenerative Braysson
cycle'},'location','best','fontsize',13)
xlabel('Pressure Ratio','fontsize',13)
ylabel('Exergy efficiency of Reheat and Regenerative Braysson cycle','fontsize',13)
legend({' T4=400^{o}C',' T4=450^{o}C',' T4=500^{o}C',' T4=550^{o}C','
T4=600^{o}C'},'location','best','fontsize',13)
%axis([1 5 0.1 0.88])
axis square
%axis([1 6 .9 1])
ax = gca;
c = ax.FontSize;
ax.FontSize = 13;

```

```

hold on
figure(13)
fig = figure(13);
u = fig.Color;
fig.Color = 'w';
%p10=plot(pr,eeffc11,'k.','markersize',8)
if t4==400
%p10(1).Marker = '*';
plot(pr,ted1,'g.','markersize',20)
end
if t4==450
%p10(1).Marker = 'o';
plot(pr,ted1,'r.','markersize',20)
end
if t4==500
%p10(1).Marker = '.';
plot(pr,ted1,'b.','markersize',20)
end
if t4==550
%p10(1).Marker = 'p';
plot(pr,ted1,'y.','markersize',20)
end
if t4==600
%p10(1).Marker = 'p';
plot(pr,ted1,'k.','markersize',20)
end
%legend({'Powerratio of Fuel cell Vs Reheat & Regenerative Braysson
cycle'},'location','best','fontsize',13)
xlabel('Pressure Ratio','fontsize',13)
ylabel('Total Exergy Destruction (KW)','fontsize',13)
legend({' T4=400^{o}C',' T4=450^{o}C',' T4=500^{o}C',' T4=550^{o}C','
T4=600^{o}C'},'location','best','fontsize',13)
%axis([1 5 0.1 0.88])
axis square
%axis([1 6 .9 1])
ax = gca;
c = ax.FontSize;
ax.FontSize = 13;
hold on
figure(14)
fig = figure(14);
u = fig.Color;
fig.Color = 'w';
if t4==400
plot(pr,NW1,'g.','markersize',20)
%p2(1).Marker = '*';
%p2(2).Marker = '*';
end
if t4==450
plot(pr,NW1,'r.','markersize',20)

```



```

%p2(1).Marker = 'o';
%p2(2).Marker = 'o';
end
if t4==500
    plot(pr,NW1,'b.','markersize',20)
%p2(1).Marker = '.';
%p2(2).Marker = '.';
end
if t4==550
    plot(pr,NW1,'y.','markersize',20)
%p2(1).Marker = 'p';
%p2(2).Marker = 'p';
end
if t4==600
    plot(pr,NW1,'k.','markersize',20)
%p2(1).Marker = 'p';
%p2(2).Marker = 'p';
end
legend({' T4=400^{o}C',' T4=450^{o}C',' T4=500^{o}C',' T4=550^{o}C','
T4=600^{o}C'},'location','best','fontsize',13)
%legend({'Energy efficiency of Hybrid cycle','Exergy efficiency of Hybrid
cycle'},'location','best','fontsize',13)
xlabel('Pressure Ratio','fontsize',13)
ylabel('Net Power output of combined system(KW) ','fontsize',13)
%axis([1 5 0.8 0.88])
axis square
ax = gca;
c = ax.FontSize;
ax.FontSize = 13;

end

%clear all

```